Chapter 14
Single-Use Bioreactors for Animal and Human Cells

Stephan C. Kaiser, Matthias Kraume, Dieter Eibl, and Regine Eibl

Abstract Single-use (SU) bioreactors are being increasingly used in production processes based on animal (i.e. mammalian and insect) and human cells. They are particularly suitable for the production of high-value products on small and medium scales, and in cases where fast and safe production is a requirement. Thus, it is not surprising that SU bioreactors have established themselves for screening studies, cell expansions, and product expressions where they are used for the production of pre-clinical and clinical samples of therapeutic antibodies and preventive vaccines. Furthermore, recent publications have revealed the potential of SU bioreactors for the production of cell therapeutics using human mesenchymal stem cells (hMSCs).

This chapter provides a perspective on current developments in SU bioreactors and their main applications. After briefly introducing the reader to the basics of SU bioreactor technology (terminology, historical milestones and characteristics compared to their reusable counterparts) an overview of the categories of currently available SU bioreactor types is provided. SU bioreactor instrumentation is then examined, before discussing well-established and novel applications of SU bioreactors for animal and human cells. This includes descriptions of the engineering characteristics of often-used types of SU bioreactors, covering wave-mixed, stirred, orbitally shaken systems and fixed-bed systems. In this context, the scaling-up of geometrically and non-geometrically similar SU bioreactors is also addressed.

Keywords Single-use bioreactors • Cell cultures • Wave-mixed bioreactors • Stirred bioreactors • Orbitally shaken bioreactors • Fixed-bed bioreactors • Sensors • Scale-up • Human cells • Animal cells • Virus-like particles • Stem cells • Microcarriers • Optical sensors • Cultivation bags • Computational fluid dynamics • Engineering characterization • Leachables/extractables • Power input • Mixing • Mass transfer

S.C. Kaiser • D. Eibl • R. Eibl (✉)
Institute of Biotechnology, School of Life Sciences and Facility Management, Zurich University of Applied Sciences, Wädenswil, Switzerland
e-mail: regine.eibl@zhaw.ch

M. Kraume
Technische Universität Berlin, Chair of Chemical and Process Engineering, Berlin, Germany

M. Al-Rubeai (ed.), *Animal Cell Culture*, Cell Engineering 9,
DOI 10.1007/978-3-319-10320-4_14

Abbreviations

1D	One-dimensional
2D	Two-dimensional
3D	Three-dimensional
bDtBPP	Bis(2,4-di-tert-butyl phenyl) phosphate
BEVS	Baculovirus expression vector system
CFD	Computational fluid dynamics
CHO	*Chinese Hamster Ovary* (cells)
CMO	Contract manufacturing organization
DoE	Design of experiments
DO	Dissolved oxygen
EDR	Energy dissipation rate
EVA	Ethylene vinyl acetate
hMSCs	Human mesenchymal stem cells
hADSCs	Human adipose-derived mesenchymal stem cells
hBM-hMSCs	Human bone(marrow)-derived mesenchymal stem cells
HPTS	Hydroxypyrene trisulfonate acid
LED	Light-emitting diode
mAbs	Monoclonal antibodies
MDCK	*Madin-Darby Canine Kidney* (cells)
MEMS	Micro-electro-mechanical systems
NK	Natural killer (cells)
PE	Polyethylene
PET	Polyethylene terephthalate
PIV	Particle image velocimetry
pO_2	Partial pressure of oxygen
pCO_2	Partial pressure of carbon dioxide
PTFE	Polytetrafluoroethylene
PVC	Polyvinylchloride
QbD	Quality by Design
RANS	Reynolds averaged Navier-Stokes (equations)
RFID	Radio-frequency identification
RT	Ruston turbine
SBI	Segment blade impeller
Sf-9	*Spodoptera frugiperda* (subclone 9)
SU	Single-use
TBPP	Tris(2,4-di-tert-butylphenyl) phosphite
VLP	Virus-like particle
WCB	Working cell bank
WVB	Working virus bank
WFI	Water for injections

Symbols

Latin symbols

Symbol	Unit	Description
a	–	Constant in Eq. 14.28
b	–	Constant in Eq. 14.28
B	m	Width of the culture bag
c	–	Constant in Eq. 14.28
C	–	Constant in Eq. 14.1
c_H	–	Mixing number
$c_{O_2,L}$	$kg \cdot m^{-3}$	Dissolved oxygen concentration
c_S	m	Impeller distance
D	m	Vessel diameter
d_0	m	Shaking diameter
$d_{B,32}$	m	Sauter diameter of gas bubbles
D_{O_2}	$m \cdot s^{-1}$	Diffusion coefficient of oxygen
d_R	m	Impeller diameter
F_G	$m^3 \cdot s^{-1}$	Gas flow rate
$Fl_{z,p}$	–	Primary axial flow number
$Fl_{z,s}$	–	Secondary axial flow number
g	$m \cdot s^{-2}$	Gravitational acceleration
H_C	$kg \cdot m^{-3} \cdot Pa^{-1}$	Henry coefficient
H_L	m	Liquid height
h_R	m	Off-bottom clearance of the impeller
k	s^{-1}	Rocking rate
k_La	s^{-1}	Specific (liquid-side) mass transfer coefficient
L_C	m	Characteristic length
N	s^{-1}	Shaking frequency
N_C	s^{-1}	Critical shaking frequency
Ne	–	Power number (Newton number)
N_R	s^{-1}	Impeller rotational speed
P	W	Power input
p_{O_2}	Pa	Partial pressure of oxygen
p_{CO_2}	Pa	Partial pressure of carbon dioxide
r	m	Radius, radial coordinate
R_r	m	Reverse point of axial flow
Re	–	Reynolds number (for stirrers)
Re_{crit}	–	Critical Reynolds number
Re_{SR}	–	Reynolds number for shaken reactors
Re_{WR}	–	Reynolds number for wave-mixed reactors (rockers)
Q_G	vvm	Aeration rate
t	s	Time
$t_{m,95\%}$	s	Mixing time (for 95 % homogeneity)
t_R	s	Hydraulic residence time

u_{tip}	$m \cdot s^{-1}$	Tip speed
V	m^3	Volume
v_G	$m \cdot s^{-1}$	Superficial gas velocity
V_G	m^3	Gas volume
V_L	m^3	Liquid (working) volume
v_z	$m \cdot s^{-1}$	Velocity in z-direction
Wo	–	Womersley number

Greek symbols

Symbol	Unit	Description
β		Parameter in Eq. 14.3
$\dot{\gamma}_{NT}$	s^{-1}	Shear gradient (local velocity gradient normal to flow direction)
Δx	m	Maximum fluid element displacement
ε_T	$m^2 \cdot s^{-3}$	Turbulent dissipation rate
η_L	$Pa \cdot s$	Liquid dynamic (molecular) viscosity
λ_e	m	Kolmogoroff microscale of turbulence
μ	h^{-1}	Specific growth rate
ν_L	$m^2 \cdot s^{-1}$	Kinematic viscosity
π	–	Circle number (≈ 3.14159265)
ρ_L	$kg \cdot m^{-3}$	Liquid density
ω	s^{-1}	Angular velocity

14.1 Introduction

In contrast to their conventional counterparts made of glass and/or stainless steel, SU bioreactors have a cultivation container fabricated from plastic materials. Generally, the cultivation vessel is pre-assembled, beta- or gamma-irradiated for sterilization and delivered by the vendor ready-to-use. After one use, it is decontaminated and discarded (Eibl et al. 2010a). While the cultivation containers in micro-, milliliter- and small liter scales are most often made of rigid polycarbonate plastics, larger systems consist of flexible two-dimensional (2D) or three-dimensional (3D) bags whose contact layers are made of polyethylene (PE) or ethylene vinyl acetate (EVA) films. In the case of cultivation bags, stainless steel trays or customized support containers, incorporating heating blankets or double jackets for temperature control, are required to shape and fix the bags.

The development of SU bioreactors was initiated by Fenwal Laboratories' (today Fresenius Kabi) invention of plastic blood bags made of polyvinylchloride (PVC) in 1953. Further milestones include the introduction of plastic flasks and dishes for routine work in cell culture laboratories during the 1960s, the invention of polystyrene multitray systems (Schwander and Rasmussen 2005) and hollow fiber bioreactors (Knazek et al. 1972) during the 1970s. Due to the availability of

different hollow fiber bioreactors (e.g. FiberCell, Amicon, Endotronics systems) (Whitford and Cadwell 2009) and two-compartment dialysis membrane bioreactors (e.g. CeLLine, MiniPerm) during the 1980s and 1990s, the production of diagnostic and therapeutic antibodies in the one and two-digit mg-range became possible (Hopkinson 1985; Falkenberg 1998; Marx 1998; Brecht 2010). The breakthrough for SU bioreactors was marked by the introduction of wave-mixed systems, the first model of which, the WAVE BIOREACTOR, was launched in the late 1990s. Its superiority for the cultivation of animal cells was demonstrated in several comparison studies (Eibl et al. 2010b), which led to the development of the WAVE BIOREACTOR 1000 and further wave-mixed bag bioreactors from various suppliers (see Sect. 14.3.1). Since the mid 2000s, different stirred bag bioreactors (see Sect. 14.3.2) have become commercially available and today, together with stirred rigid bioreactors (see Sect. 14.3.2), make the largest group of SU bioreactors. Various types of bioreactors, which differ from the wave-mixed and stirred mixing principle (see Sect. 14.2.1), are also currently available.

If SU bioreactors are selected properly and operated correctly, more flexible, safer, greener, cheaper and faster production processes can be achieved compared to reusable bioreactors (Aranha 2004; Ott 2011). In fact, steam sterilization prior to inoculation and costly, time and labor intensive cleaning procedures become obsolete, eliminating the need for aggressive, corrosive cleaning agents and water for injections (WFI) used in final rinse cycles. Furthermore, the need to validate the cleaning processes and the risks of cross contamination in multiproduct manufacturing facilities are also reduced, which enables more flexible and quicker product changes, as well as reducing costs.

However, cell growth and product quality/quantity can be affected by chemical, biological and physical properties of SU cultivation containers. This has already been demonstrated for bags made of PE films used for cultivations with serum-free, protein-free and chemically defined culture media (Altaras et al. 2007; Kadarusman et al. 2005). The strength of this effect depends on several factors, including the sensitivity of the production cell line, the components contained in the culture media, the initial cell density and storage time of the PE bags. As shown in Fig. 14.1, the film of the bag consists of multiple layers.

Due to the absence of serum albumins as carrier molecules in serum-free culture media, interactions between media components (e.g. cholesterol and fatty acids) and the contact layer may occur, which can limit cell growth or inhibit product secretion (Kadarusman et al. 2005). The most important concerns are related to cytotoxic leachables, which migrate from the film material into the culture broth and inhibit cell proliferation and product expression (Horvath et al. 2013; Wood et al. 2013). Using *Chinese Hamster Ovary* (CHO) cell lines, Hammond et al. (2013) identified bis(2,4-di-tert-butyl phenyl) phosphate (bDtBPP) as a potential leachable that decreases mitochondrial membrane potential and suppresses cell growth at concentrations as low as 0.1 $mg \cdot L^{-1}$. This compound is generated during gamma irradiation (25–45 kGy) by the degradation of tris(2,4-di-tertbutylphenyl) phosphite (TBPP, often referred to by its trade name Irgafos 168), an antioxidant stabilizer that is commonly added to PE resins. Consequently,

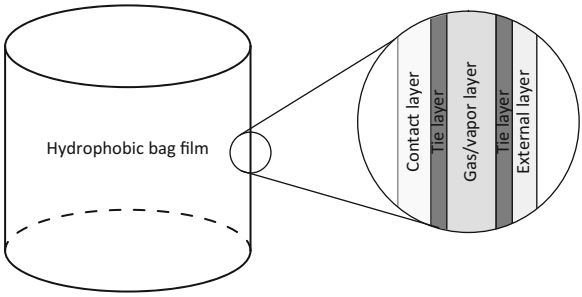

Fig. 14.1 Typical composition of a multilayer bag used as a bioreactor container. The functional layers in a multilayer film include (1) the contact layer, which provides an inert surface, (2) the gas/vapor barrier layer, which limits the diffusion of gasses and vapors and is typically made of Ethylene vinyl alcohol, (3) the external layer, which improves the mechanical performance of the film, and (4) the tie layers between the previously mentioned layers, which bond them together through physicochemical interactions

in-house performance studies, such as the recently published DECHEMA bag test study (Eibl et al. 2014b), with cultivation bags and applied production cell lines / cultivation systems are required to identify potential cytotoxic leaching if SU bioreactors are to be implemented successfully. Consistent, complete and traceable quality control of bag supplies helps to reduce the requirement for bag tests at customers sites and improves the acceptance of commercially available SU systems in production processes.

14.2 Overview of Current SU Bioreactors on the Market

Due to the rapid development of SU bioreactors in the last two decades, users can now choose between a multitude of types which differ in the design of the cultivation container, instrumentation and scale. Based on their design, SU bioreactors can be distinguished as follows: flexible bags, rigid dishes, tubes, cartridges, flasks and vessels. Small scale systems mostly use either very little or no instrumentation. But as size increases systems are equipped with sensors to monitor and control key parameters (see Sect. 14.2.2). In general, these systems are connected to a control unit and no external equipment, such as incubators, is required to maintain optimal process conditions for the production organisms.

Currently SU bioreactors with working volumes of up to 2,000 L are commercially available (Löffelholz et al. 2013a). Eibl and Eibl (2010) distinguish between small-volume systems (screening scale), medium-volume systems (benchtop and pilot scale) and large-volume systems (production scale). They presented an approach for categorization based on power input and classified SU bioreactors into static and dynamic systems. Static systems, such as t-flasks and multilayer flasks, are exclusively used on small and medium scales, because mass transfer is

limited, leading to lower cell densities and product titers compared to dynamic systems.

14.2.1 Categories/Classes of SU Bioreactors

In Fig. 14.2, an approach to the categorization of dynamic SU bioreactors according to their mixing and power input, which has been developed by the DECHEMA's temporary working group "single-use technology in biopharmaceutical manufacture", is presented below.

The largest group of SU bioreactors is mechanically driven which can be further subdivided in stirred, oscillating and orbitally shaken systems. Stirred SU bioreactors (see Sects. 14.3.2 and 14.3.3) consist of cylindrical or cube-shaped vessels and are mostly bubble aerated. Centrically mounted, rotating stirrers are predominantly used, hence baffling is desirable, in particular for larger scale implementations, in order to improve mixing. However, under the majority of operating conditions baffles are not required. The stirrers are usually magnetically driven and mechanically coupled to seal the shaft. Tumbling stirrers, as used in the Nucleo Bioreactor from ATMI (max. 1,000 L culture volume), are less common, although they provide thorough mixing at low specific power inputs (Zambeaux et al. 2007). In oscillating systems, mixing is driven by horizontal oscillation (wave-mixed bag bioreactors, max. 500 L culture volume, Sect. 14.3.1), by vertical oscillatory rotation (BayShake bioreactor, max. 1,000 L culture volume (Kauling et al. 2013)) or by vibrating perforated discs (Saltus Vibromix bioreactor, max. 1,000 L culture volume (Werner et al. 2010b)). Similar to the orbitally shaken SU bioreactors (max. 200 L culture volume, Sect. 14.3.4), oscillating systems using either bubble or surface aeration are available.

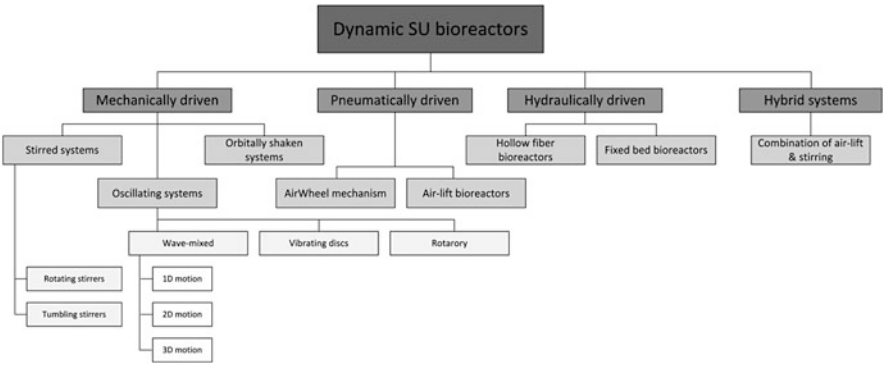

Fig. 14.2 Power input-based categorization of dynamic SU bioreactors for animal and human cells. The classification, produced by the DECHEMA's temporary working group "single-use technology in biopharmaceutical manufacture", distinguishes between mechanically driven, pneumatically driven, hydraulically driven and hybrid driven SU bioreactors

The mixing and aeration of pneumatically driven bioreactors is achieved by direct gassing of the liquid with air or gas by an aeration device integrated into the cultivation bag. An example is the PBS bioreactor series (max. 2,500 L culture volume (Schultz and Giroux 2011)), which is agitated by Air-Wheel® technology and aerated through a dual sparger (Kim et al. 2013; Lee et al. 2010). The hybrid CellMaker Plus system (max. 50 L culture volume) from Cellexus combines the principles of a bubble column and stirring (Shukla and Gottschalk 2013).

As shown in Sect. 14.4, microcarriers can be used in mechanically and pneumatically driven bioreactors if the applied cell lines require immobilization to achieve desired product quantities and qualities. Alternatively, hydraulically driven hollow fiber bioreactors (max. 2.1 m^2 growth surface) incorporating a pump or the recently introduced fixed SU bed bioreactors (max. 500 m^2 growth surface, Sect. 14.3.5) can be used (Brecht 2010; Kilian 2013).

14.2.2 Instrumentation of SU Bioreactors

Instrumented bioreactors either operate with in-situ sensors, which are in direct contact with the process fluid and therefore have to be sterilizable, or ex-situ sensors which allow non-invasive control. Sterilizability of ex-situ sensors, such as optical sensors that take measurements through a transparent window or classical sensors that are fitted outside of the sterile barrier (Lindner et al. 2010) is not an issue. Important parameters for process control and automation that can be monitored in traditional cell culture bioreactors include primarily physical properties, such as temperature, pH value, dissolved oxygen (DO) and carbon dioxide concentration, stirrer or rocking speed, gas and liquid flow rates, pressure, foam/level and vessel weight. Furthermore, advanced parameters such as power input, off-gas composition and biological parameters (including cell density, concentrations of substrates, products and metabolites, redox potential, conductivity etc.) are monitored in heavily instrumented systems, which are mostly found in R&D environments. However, currently only a few SU solutions are commercially available for determining advanced parameters (see Table 14.1).

The first challenge to overcome when implementing SU sensors in bags or rigid plastic vessels is related to the beta- or gamma-sterilization processes (Bernard et al. 2009). The sensor has to be inserted into the bag and must withstand the sterilization process without loss of functionality and sensitivity. Furthermore, the sensors must be inexpensive, if they are to be disposable. Alternatively, traditional probes can be used, but these have to be cleaned and sterilized externally and are subsequently connected to the SU bioreactor via aseptic couplings. An example of this concept can be seen in the stirred S.U.B. from Thermo Fisher, where autoclavable probe assemblies using Kleenpak connectors are used.

The most important parameters to be measured in SU bioreactors are DO and pH. Physically similar sensor designs and apparatus are used to measure both parameters, although the optics, chemistry of the sensor patch and methodologies

Table 14.1 Selected available SU sensors and their specifications for the measurement of biological and physical parameters

Parameter	Working principle	Manufacturer/ vendor	Specifications
Dissolved oxygen	Optical (fiber optical)	PreSens[a]	Measurement range 0–100 % O_2 (detection limit: 0.03 % O_2)
			Resolution ±0.1 % O_2 at 20.9 % O_2 (±0.01 % O_2 at 0.21 % O_2)
			Drift at 0 % O_2 <0.03 % O_2 within 30 days (sampling interval: 1 min)
		Ocean Optics, Inc.[d]	Measurement range 0–100 % O_2
			Detection limit: 0.05 % O_2 in gas and 0.02 ppm in liquid
			Resolution ±0.05 % at room temperature
	Optical (LED and large area photodiode)	Finesse Solutions, Inc.	Measurement range: ~ 0–52.5 % O_2 (250 % air-saturation)
			Precision: 0.55 % or <3 % (whichever is greater) of reading at O_2 levels <21 %
			Operating temperature: 4–45 °C
			Accuracy at 20 °C: <±1 % at 20.95 % O_2
pH value	Potentiometric	Sartorius Stedim Biotech SA and Metroglas	Measurement range: 0–11 pH
			±0.1 pH units precision (pH 2–9)
			Response time: <60 s (until drift <0.6 $mV \cdot min^{-1}$)
	Optical (fiber optical)	PreSens	Measurement range: 5.5–8.5 pH
			Response time (t_{90})[b]: <120 s
			Resolution at $pH = 7 \pm 0.01$ pH
			Accuracy at $pH = 7 \pm 0.05$ sensor spot calibration
			Drift at $pH = 7 < 0.005$ pH per day (sampling interval of 60 s)
		Ocean Optics, Inc.	Measurement range: 5.0–9.0 pH

(continued)

Table 14.1 (continued)

Parameter	Working principle	Manufacturer/ vendor	Specifications
	Optical (LED and large area photodiode)	Finesse Solutions, Inc.	Measuring range pH 5.5–8.5
			Rel. accuracy ±0.1 pH unit over ±0.5 pH range centered at 1-point stand. pH value
			Response time (t_{90}, agitated): <90 s
			Drift: <0.05 pH units over 21 days (sampling rate: once every 5 s)
Dissolved carbon dioxide	Optical (fiber optical)	PreSens	Measurement range: 1–25 % CO_2 at atmospheric pressure (1,013.15 hPa)
			Response time (t_{90}) at 20 °C: <3 min for changes from 2 % to 5 % pCO_2
			Resolution at 20 °C: ±0.06 % at 2 % CO_2 and ±0.15 % at 6 % CO_2
			Drift at 37 °C in a CO_2 incubator with 100 % rel. hum.: <5 % of reading per week
Pressure	Piezoresistive effect (electrical resistance of a metal or semiconductor caused by mechanical strain)	PendoTECH	−0.48 to 5.2 bar measurement range
			15–40 °C operating temperature
			<±5 % measurement accuracy
			Sizes: Luer, ¼″–1″ hose barb
		SciLog	−0.34 to 4.1 bar measurement range
			±20 mbar measurement accuracy
			Sizes: Luer, 3/8″–1/2″ hose barb, ¾″–1″ tri-clover
		Finesse Solutions, Inc.	0–0.48 bar measurement range
			±1.4 mbar measurement accuracy (at 25 °C, including drift 21 days)
			±1.4 mbar sensor drift over 21 days
	RFID-tag-based transducer with pressure-sensitive membrane[c]	GE Healthcare	−0.34 to 2.3 bar
			±17 mbar measurement accuracy

(continued)

Table 14.1 (continued)

Parameter	Working principle	Manufacturer/ vendor	Specifications
Flow rate	Ultrasonic	Levitronix	Measurement range[d]: 0–80 $L \cdot min^{-1}$
			Accuracy of $\pm 0.188\ L \cdot min^{-1}$ below 1 $m \cdot s^{-1}$ and ±1 % above 1 $m \cdot s^{-1}$
	Infra-red reflection	Equflow	Measurement range[d]: 0.1–20 $L \cdot min^{-1}$
			Accuracy: 1 % of reading
	Coriolis	PendoTech	Measurement range[d]: 5–24,000 $g \cdot min^{-1}$
			Accuracy of ±1 % of rate + zero offset stability (0.06–20 $g \cdot min^{-1}$)
			Max. operating pressure: 80–120 psig
Glucose, Lactate, Glutamine	Enzymatic oxidation and electron transfer from analyte to electrode (anode)	CITsens Bio	Measurement range: 1–60 $mmol \cdot L^{-1}$
			Resolution: 0.1 $mmol \cdot L^{-1}$
			Detection limit: 1 $mmol \cdot L^{-1}$
			Precision: $\pm 1\ mmol \cdot L^{-1}$
Conductivity	4-electrode conductivity cell	SciLog	Measurement range: 1–200 $mS \cdot cm^{-1}$
			Accuracy: $\pm 2.5\ mS \cdot cm^{-1}$ of full range
		PendoTECH	Measurement range: 0.1–50 $mS \cdot cm^{-1}$
			Temperature normalization to 25 °C
			Accuracy: $\pm 0.1\ mS \cdot cm^{-1}$ from 0.1 to 2 $mS \cdot cm^{-1}$ and ±5 % of reading at 2–50 $mS \cdot cm^{-1}$

[a]Data depend on the sensor material
[c]Equilibrated sensor kept in well stirred solution at 37 °C
[c]Under development
[d]Different sensor sizes available

differ. The majority of SU sensors for measuring DO are based on the principle that oxygen quenches the fluorescence of a fluorophore in a dynamic and well-defined manner (see Fig. 14.3). The sensing patch is typically illuminated by one or more properly filtered light sources (e.g. LEDs). The dye, commonly a ruthenium-based or platinum-based fluorophore with a lifetime of longer than 10 ns that is incorporated into a silicone matrix, emits light that differs from the incident light in wavelength, phase, and intensity. If oxygen is present near the fluorophore, the oxygen molecule receives the excess energy via non-radiative transfer, resulting in

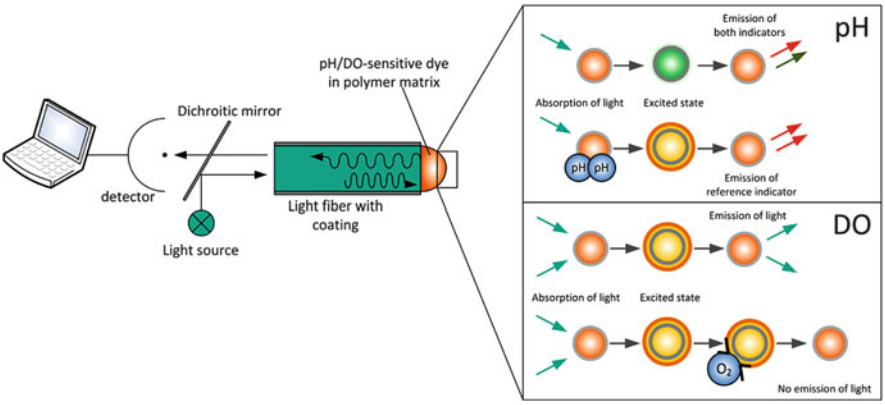

Fig. 14.3 Schematic of the general setup of a fiber-optic sensor with a dichroic mirror. The principle of fluorescence dependent pH and DO measurement are also provided (Adapted from Lindner et al. (2010) and PreSens' website www.presens.de)

a reduction or quenching of the fluorescent signal. The magnitude of the phase shift and intensity difference depends on the DO level in the surrounding liquid. A photomultiplier or photodiode is used to capture the emitted fluorescence after separating it from the excitation light using a dichroic mirror (Glindkamp et al. 2010). Because of possible errors caused by ambient light conditions, background noise and changes in incident intensity, fluorescent intensity is less desirable than phase shift as the primary measurement variable. Despite the fact that phase shift is preferred, it is more difficult to measure electronically (Qualitz 2009).

In contrast to oxygen-consuming Clark electrodes, optical sensors can be used in diffusion limited zones where electrochemical probes would decrease the oxygen concentration (Armstrong 1994). Furthermore, optical sensors can be miniaturized, which enables measurements to be taken in small volumes of less than 1 mL (Rao et al. 2009). Sensing electronics are extremely stable and only need to be calibrated once a year (Qualitz 2009). Due to the more laborious calibration procedures required for the proper use of conventional probes, the setup of optical sensors is substantially less time-consuming than for conventional probes, since they arrive pre-calibrated from the vendor. Commercially available optical oxygen sensors, e.g. from PreSens (Germany), Ocean Optics, Inc. (USA) and Sartorius Stedim (Germany), are irradiatable without loss of sensitivity. The measurement ranges of these sensors are between 0 % and 100 % pO_2 (see Table 14.1).

Long-term stability is a key requirement of optical sensors and should be at least guaranteed for the shelf-life of the cultivation bags. However, limited long-term process stability, which is mainly affected by photobleaching, is the most pronounced disadvantage of optical sensors. This can, however, be compensated for by modifying the dye. According to Lai et al. (2004), the photostability of highly electron-deficient, multiple fluorinated platinum porphyrins is significantly enhanced compared to non-substituted fluorophore. As an alternative approach,

optical filters are integrated into the large area photodiodes utilized in TruFluor™ sensors provided by Finesse Solutions, Inc. This reduces the light intensity required and, therefore, minimizes photo-degradation of the active sensing element. The sheaths of both TruFluor™ DO and TruFluor™ pH sensors can be pre-inserted into SU bioreactor bag ports prior to gamma-sterilization (Paldus and Selker 2010).

Fiber-optic pH sensors contain either fluorescence- or absorption-based pH indicators. The latter include phenol red and cresol red indicators (Mills et al. 1992). Frequently used fluorescing dyes include fluorescein derivatives and hydroxypyrene trisulfonate acid (HPTS) (Munkholm et al. 1988; Mills and Chang 1993; Fritzsche et al. 2007), which exhibit two excitation wavelengths corresponding to the acid and its conjugate base. The pH can be determined from the ratio of emission intensities using a pair of high intensity LEDs (one ultraviolet and one blue) that excite the patch. While fiber-optic pH sensors can – like other chemosensors – be miniaturized and offer short response times, disadvantages of fluorescence-based pH sensors include cross-sensitivity to ionic strength and limited measurement ranges (about 3 pH units).

A wider pH range was obtained by Li et al. (2006), who immobilized modified fluorescent aminophenylcorroles in a sol-gel matrix. A recently introduced SU pH sensor, which was jointly developed by Sartorius Stedim Biotech SA and Metroglas and utilizes a potentiometric pH measurement, offers a range of pH measurements from pH 0–11 with ±0.1 precision (Bernard et al. 2009). However, the pH sensor must be kept in a wet environment during storage, before and after gamma sterilization. For this purpose, a patented encapsulation device was developed that enables the insertion into Flexel® 3D media bags without affecting sterility. Specific gels were chosen for both the internal and external reference electrolytes, which enable measurement in any orientation, while the short probe body simplifies packaging and handling (Bernard et al. 2009).

Fiber-optic sensors can also be utilized for the measurement of dissolved carbon dioxide (pCO_2) (Uttamlal and Walt 1995). Based on the Severinghaus pCO_2 electrode principle, the sensor consists of a pH sensitive dye (e.g. HPTS) in an HCO_3^- buffer solution. This is encapsulated in an expanded polytetrafluoroethylene (PTFE) support, which is held at the distal end of an optical fiber by a gas permeable membrane. A pH change in the indicator solution, which is related to the pCO_2 by the Henderson-Hasselbalch equation, is produced by CO_2 crossing the membrane. PreSens pCO_2 sensors utilize the Dual Lifetime Referencing method as an internal reference, where the signals of an analyte sensitive indicator and an inert reference indicator with very different luminescence lifetimes are superimposed on one another (Klimant 2003).

Pressure is another crucial, safety-related process parameter, since an overpressure situation, e.g. resulting from a clogged vent filter, can easily rupture the cultivation bags, resulting in batch loss. However, SU bioreactors are often not compatible with traditional stainless steel pressure gauges. While the pressure in some systems is controlled by a re-usable pressure sensor outside of the sterile barrier, static and dynamic pressures of gases or liquids in SU bioreactors can be accurately measured by low-cost micro-electro-mechanical systems (MEMS) that

are based on piezoresistive pressure measurements. The sensor elements are typically integrated in a Wheatstone bridge circuit, through which an applied pressure gives a proportional output voltage (Bink and Furey 2010). Pressure sensors from PendoTech and SciLog® for measuring the pressure inside tubing are commercially available and have similar measurement ranges of up to 5.2 bar. For small-scale systems, sensors originally designed for medical applications can be integrated into flexible tubing in a flow-through mode using Luer or hose barb adapters. Larger diameters also have tri-clover connections. The repeatability, accuracy, and robustness of the MEMS in these sensors were found to be satisfactory (Clark and Furey 2007). Sensors are accurate to 20 mbar for pressures up to 1 bar and 2.5 % of the reading value for pressures between 1 and 1.51 bar. Since the signal from the sensors is not a traditional field output signal, such as 0–20 mA or 0–10 V, an intermediate device is required to display and transmit the sensor readings to a process control system (Furey 2007).

To measure the pressure in the headspace of flexible bags, the TruTorr™ provided by Finesse Solutions, Inc. can be used. Based on integrated, gamma radiation-resistant memory chip technology, the sensor compensates for temperature and is self-calibrated for immediate use.

In the future, an alternative to piezoresistive sensors may be provided by recently developed passive radio-frequency identification (RFID) sensors (Surman et al. 2011). They consist of a pressure sensitive flexible membrane, an RFID-tag-based transducer and a layer that modulates the electromagnetic field generated in the RFID sensor antenna. Multivariate analysis of the measured impedance of the sensor provides temperature-independent pressure response. However, no commercial solution for pressure measurements in SU equipment based on RFID is currently available.

Further process parameters detectable by SU sensors include conductivity (SciLog, PendoTECH), flow rates (LeviFlow), capacitance (Fogale Nanotech, Aber Instruments) and total protein concentration (Schneditz et al. 1989). The conductivity sensors provided by both SciLog and PendoTECH are pre-calibrated according to pre-determined cell constants, which are stored on each sensor's chip for out-of-the-box, plug and play use. Flow rates are most commonly measured by ultrasonic signals, where the ultrasonic wave is accelerated or decelerated depending on the flow direction, thus providing a direct measure of the liquid velocity, as in the LeviFlow® sensors provided by the Levitronix GmbH. In contrast, Equflow flow sensors are based on infra-red reflection signals that are monitored by an ultra-light-weight turbine rotor. PendoTech also offers a SU Coriolis flow meter.

Information on biomass concentration can be obtained using turbidity. The use of backscattering light can increase the range of linear correlation for higher particle concentrations. However, while turbidity sensors only give a measure of total biomass concentration, capacitance sensors can provide specific information on viable cell mass. The latter are based on the fact that the non-conducting (intact) cell membranes allow a build-up of charge in an alternating electrical field.

Furthermore, the capacitance signal is not sensitive to gas bubbles, cell debris and other particles in suspension (www.fogalebiotech.com).

To monitor metabolization of glucose, glutamate and/or lactate during cultivation, CITSens Bio sensors can be used, which are based on an enzymatic oxidation process and electron transfer from the analytes to the anode (Spichiger and Spichiger-Keller 2010). In contrast to a number of alternative sensors on the market, where hydrogen peroxide production is measured and, therefore, sufficient oxygen is required, the function of CITSens Bio sensors is not affected by oxygen concentration. Furthermore, the by-products that are produced are of exceptionally low concentrations. Depending on the bioreactor, the sensors are built into the original cap of T-flasks, roller flasks, shake flasks or bag-reactors and are gamma-sterilized before being delivered to the customer. However, storability is limited to about 21 days (15 days for lactate) as a result of sensor instability (the specified storage time at 5 °C is 6 month) (www.c-cit.ch).

A special feature for integrating SU and/or conventional sensors is the Mobius® SensorReady technology, which is implemented in Mobius® CellReady 50 L and 250 L bioreactors (see Sect. 14.3.3). It consists of an external loop that enables configurable and flexible mounting of sensors. The culture broth is pumped from and to the vessel using a Levitronix® centrifugal-type pump, operated at $3\ \mathrm{L} \cdot \mathrm{min}^{-1}$ (pump speed 2,000 rpm). CFD studies have revealed significantly lower energy dissipation rates (EDRs) inside the pump ($< 5 \cdot 10^5\ \mathrm{W} \cdot \mathrm{m}^{-3}$) than critical thresholds responsible for lethal cell responses that have been reported in the literature (Mollet et al. 2007; Godoy-Silva et al. 2009) and determined experimentally by the manufacturer for four different cell lines (Kittredge et al. 2011). Furthermore, the general applicability for microcarrier based cultivations (MDCK cultivated with SoloHill® Collagen microcarriers) has also been demonstrated (McGlothlen et al. 2013).

14.3 Often Used Instrumented Dynamic SU Bioreactors and Their Engineering Characteristics

As described in Sect. 14.2.1, the most often used SU bioreactors are mechanically driven versions, which are wave-mixed, stirred, or orbitally shaken. Furthermore, new developments, such as fixed bed bioreactors, have more recently entered the market. However, the size of SU bioreactors is still limited to approximately 2,000 L. The upper limits mainly result from manufacturing and bioengineering limitations, in particular related to mixing and mass transfer. The following sections describe selected bioreactors and their engineering characteristics that are relevant for biopharmaceutical production processes.

14.3.1 Wave-Mixed Bag Bioreactors

The first wave-mixed bioreactors that entered laboratories in the 1990s had rocker platforms. The rocker platform had a periodic, 1D oscillatory motion that moved a partially filled, pillow shaped bag (Singh 2001). The wave inside the bag is induced by the platform motion, whereas the wave characteristics depend on the bag shape/geometry (this differs according to scale), the rocking angle, the rocking rate, the filling volume and the fluid properties, i.e. liquid density and viscosity (Eibl and Eibl 2009a; Eibl et al. 2010b). Today, the 1D oscillatory concept is used in commercially available wave-mixed systems, including the Wave Bioreactor (GE Healthcare), the BIOSTAT® CultiBag RM (Sartorius Stedim Biotech), the AppliFlex bioreactor (Applikon) and the SmartRocker^{TM} (Finesse Solutions, Inc.). Major differences between these bioreactors are related to their culture bag designs (i.e. shape, dimensions, scale, film material, installations), control units, rocker platforms and instrumentation.

Both the BIOSTAT® CultiBag RM and the Wave Bioreactor Cellbags are available with optionally integrated perfusion membranes for cell retention. While the membrane in the BIOSTAT® CultiBag RM (1.2 μm and 1,070 or 1,275 cm^2 surface area) is fixed to the bottom of the bag, the Wave Bioreactor incorporates a floating filter with a flat cell-retentive membrane (0.7 μm pore size and 100 or 180 cm^2 surface area) (Tang et al. 2007). Hence, very high cell densities are achievable with 1D motion wave-mixed systems (Tang et al. 2007; Adams et al. 2011).

The fluid flow inside the 1D motion bags can be characterized by a modified Reynolds Re_{WR} number given by Eq. 14.1, which is determined using the working volume (V_L), the width of the culture bag (B), the liquid level (H), the rocking rate (k), the kinematic viscosity of the liquid (v_L), and an empirical constant that depends on the bag type (C). According to the definition provided by channel flows, turbulent conditions occur above a critical Re (Re_{crit}) of 1,000 (Eibl et al. 2010b).

$$\mathrm{Re}_{WR} = \frac{V_L \cdot k \cdot C}{v_L \cdot (2H_L + B)} \tag{14.1}$$

In contrast, the non-dimensional Womersley number (Wo), a classical non-dimensional number, and a parameter β were used to quantify the unsteady nature of the flows (Oncül et al. 2009). Wo is expressed by Eq. 14.2, where L_C denotes the characteristic length scale of the flow (i.e. liquid level in the culture bags) and ω is the angular velocity of the oscillations.

$$Wo = \frac{L_C}{2} \cdot \sqrt{\frac{\omega \cdot \rho_L}{\eta_L}} \tag{14.2}$$

The parameter β is obtained from Eq. 14.3, where Δx represents the maximum fluid element displacement in the vessel during one rocking cycle, which is hard to determine experimentally. It has been stated that turbulent conditions appear in oscillating flows when β exceeds 700 for Wo greater than 8.5 (Oncül et al. 2009).

$$\beta = \Delta x \cdot \sqrt{\frac{\omega}{\nu_L}} \tag{14.3}$$

The wave motion promotes bulk mixing, off-bottom suspension of cells and particles, bubble-free surface aeration and reduces foaming and flotation compared to stirred cell culture bioreactors (Eibl et al. 2010b). Reported k_La values are in the range of 0.5 and 24.1 h^{-1} (see Table 14.2), making them suitable for cultures with low and medium oxygen demands (Eibl and Eibl 2009a). Detailed comparisons of different cultivation bags is difficult because of non-comparable operational conditions and measurement techniques. Furthermore, it should be emphasized that the given data include limit values ($k_La < 5$ h^{-1}), which are not recommended for the cultivation of human and animal cell lines.

In general, oxygen mass transfer in a given bag geometry has been found to depend on the rocking rate, rocking angle and the filling level. Hence, Eq. 14.4 can be determined from data obtained from a BIOSTAT® CultiBag 2 L (Imseng 2011).

$$k_\mathrm{L}a \propto {V_\mathrm{L}}^{2.7} \tag{14.4}$$

It should be emphasized that this equation is only valid for this bag size. At a given volume, small changes in the rocking rate and/or rocking angle can increase the k_La more significantly than raising the aeration rate (Eibl et al. 2010b). Nevertheless, contrary data have been reported with respect to aeration rate by using the gassing-out method to determine the k_La (Singh 1999; Knevelman et al. 2002; Imseng 2011; Fietz 2013). Following the conventional definition from submerse aeration, the aeration rate is defined as the air flow rate related to the liquid volume (F_G/V_L), given in vvm (volume gas per volume liquid and minute). Air flow rate has been found to have a strong influence on the k_La value, in the BIOSTAT® CultiBag 2 L bioreactor working with different filling volumes of between 0.3 and 0.5 L up to a critical flow rate of 0.15 L · min^{-1}, corresponding to 0.3 vvm at 0.5 L, as indicated by Eq. 14.5 (Imseng 2011).

$$k_La \propto {F_G}^{1.22} \tag{14.5}$$

This correlation is consistent with measurements provided by Singh (1999), who found that the aeration rate had a significant influence in the Wave 2 L bag when filled to its maximum working volume. The k_La at 30 rpm was increased from 2.0 to 2.7 h^{-1} by increasing the aeration rate fivefold (0.01–0.05 vvm), even though this results in a different exponent in Eq. 14.5. Furthermore, by correlating data reported by Singh (1999) for Wave 20 L bags, an exponent of F_G of 1.29 can be obtained. However, it should be emphasized that, following the traditional definition of the

Table 14.2 Summary of reported k_La values for selected operating conditions in 1D rocker-type SU bioreactors. The given data include limit values ($k_La < 5$ h^{-1}), which are not recommended for the cultivation of human and animal cell lines

	Working volume (L)	Rocking rate (rpm)	Rocking angle (°)	Aeration rate (vvm)	k_La value (h^{-1})	Reference
Wave Bioreactor 2 L	1	5	n.d.	0.05	2.0	Singh (1999)
	1	10	n.d.	0.05	2.1	
	1	20	n.d.	0.05	2.8	
	1	30	n.d.	0.05	2.7	
Wave Bioreactor 20 L	10	5	n.d.	0.1	0.7	Singh (1999)
	10	10	n.d.	0.1	1.4	
	10	20	n.d.	0.1	2.7	
	10	30	n.d.	0.1	3.9	
BIOSTAT® CultiBag RM 2 L (basic)	0.2	8	6	0.1	0.5	Imseng (2011)
	0.2	8	6	0.2	1.4	
	0.2	8	6	0.4	3.4	
	0.35	8	6	0.4	5.2	
	0.5	8	6	0.4	4.1	
BIOSTAT® CultiBag RM 20 L (optical)	2	27	7	0.05	19.4	Fietz (2013)
	2	27	7	0.075	17.4	
	2	27	7	0.1	18.9	
	10	6	10	0.02	1.1	
	10	6	10	0.25	1.1	
	10	30	5	0.25	15.3	
AppliFlex 20 L	2.5	16	2	0.5	5.1	Müller (2010)
	5	16	7	0.5	10.2	
	5	24	7	0.5	19.1	
	5	24	9	0.5	22	
	5	24	11	0.5	24.1	

n.d. not defined

k_La value (provided, for example, by Zlokarnik (1999)), the overall mass transfer can be expected to be limited by the resistance at the liquid side of the gas-liquid interface. It is unlikely that this resistance is influenced by the surface aeration (as long as no significant surface turbulence is induced by the air flow).

In agreement with this assumption (but in contrast to previous findings), data determined in BIOSTAT® CultiBags RM 20 L and 200 L revealed that the air flow rate had a negligible influence on the k_La value (Knevelman et al. 2002; Fietz 2013). This was demonstrated using the gassing-out method, with nitrogen, and the sulfite method, as described by (Garcia-Ochoa and Gomez 2009). It has been suggested that the apparent dependency on the air flow rate resulted from varying oxygen partial pressures (p_{O_2}) in the bag head space, after eliminating the dissolved oxygen by introducing nitrogen during the classical gassing-out method (Fietz 2013). According to Henry's law both parameters are related by the Henry coefficient H_C (see Eq. 14.6).

$$c_{O_2,L} = H_C \cdot p_{O_2} \tag{14.6}$$

A time-depended DO saturation concentration (see Eq. 14.7) can be estimated, assuming an ideally mixed bag head space. This was confirmed by measuring the gas residence time distribution using a BlueInOne gas analyzer (BlueSens).

$$\frac{dc_{O_2,L}(t)}{dt} = k_L a \cdot \left(H_C \cdot p_{O_2}(t) - c_{O_2,L}\right) \tag{14.7}$$

It should be noted, that there is doubt about whether ideally mixed conditions occur in the bag head space because of the close proximity of the gas inlets and outlets in most wave-mixed cultivation bags. Nevertheless, very good agreement between theoretical response profiles and experimental data was found for both the residence time distribution and the mean residence time (Eq. 14.8) of the oxygen used as tracer in the exhaust air.

$$t_R = \frac{V_G}{F_G} \tag{14.8}$$

This was tested for a wide range of aeration rates (0.01–0.1 vvm) and filling volumes (2–10 L) in a BIOSTAT® CultiBag RM 20 L bag (Fietz 2013). In conclusion, the experimental methods for k_La determination should be carefully taken into account when comparing literature data. Based on our experience, when using the classical gassing-out method, it is recommended, that the nitrogen in the bag's headspace, which influences the oxygen saturation concentration, should be eliminated.

According to Singh (1999), mixing times in the Wave bioreactor determined by injecting a fluorescent dye and videotaping the dispersion of the dye ranged from 5 to 10 s for working volumes of 10 L (in 20 L bags) and were up to 60 s for volumes of 100 L (in 200 L bags). These are satisfactory values for cell culture bioreactors. Using 2.5 and 5 L working volumes in an AppliFlex® bioreactor (20 L total volume), mixing times of between 4 and 14 s were determined (Müller 2010). A wider range was reported by Eibl and Eibl (2009b), where determined mixing times were between 10 s and ≈ 1,400 s in the Wave bioreactor for scales of up to 100 L with filling levels of between 40 % and 50 %. Not entirely surprisingly, the most ineffective mixing was observed at the lowest possible rocking rate, rocking angle and maximum filling level of 50 %, while the mixing could be improved by increasing the rocking rate and/or the rocking angle and by decreasing the filling volume. The most ineffective mixing (40 s to ≈ 1,400 s) was found in 20 L bags, whereas the mixing times were surprisingly similar or even longer than those at the 100 L scale. In contrast, the most effective mixing (9–264 s) was achieved in 2 L bags (Eibl and Eibl 2009b).

For these bags, the specific power inputs (P/V) were determined by calculating the momentum achieved by both analytical and graphical determination of the point of gravity of the culture bag and the surface area of the fluid (Eibl et al. 2010b).

Using the recommended minimum filling levels (0.2 L), specific power inputs of up to $\approx 560\ W \cdot m^{-3}$ were determined at a rocking rate of 30 rpm and rocking angle of 10°. However, significantly lower power inputs of $\approx 70\ W \cdot m^{-3}$ have been reported at the maximum filling level (1 L at 30 rpm and 10°). For identical operational conditions, somewhat higher values ($\approx 150\ W \cdot m^{-3}$) were predicted by Computational fluid dynamics (CFD) simulations, which, in contrast to the experimental method, take the dynamic energy of the fluid into account (Löffelholz et al. 2010). Nevertheless, both methods revealed that the power input for a given filling volume is directly proportional to the rocking rate and rocking angle. It should be noted, that operational parameters must be evaluated together. For example, by filling BIOSTAT® CultiBag RM 200 L bags to 50 %, specific power inputs of $\approx 150\ W \cdot m^{-3}$ can be achieved by either setting a rocking rate of 30 rpm and rocking angle of 6.5° or a rocking rate of 20 rpm and a rocking angle of 9° (Löffelholz et al. 2010). Interestingly, the power input levels out and may even slightly decrease for certain operational conditions (Eibl et al. 2010b).

In contrast to the bag bioreactors mentioned above, the CELL-tainer® SU bioreactor employs a 2D-motion that combines the vertical rocking motion with a horizontal translation. Even though there are some doubts on the reliability of the reported data, this combination may allow significantly higher oxygen mass transfer rates to be achieved. Thus, k_La values of up to $600\ h^{-1}$ for 15 L working volume have been reported. Even with a 150 L volume k_La values of up to $300\ h^{-1}$ have been found (Oosterhuis et al. 2013). For these operational conditions, the specific power input is about $3\ kW \cdot m^{-3}$, which is comparable to standard stirred bioreactors that are used for microbial cultures (Oosterhuis and van der Heiden 2010). Thus, the cultivation of fast-growing microorganisms with a high oxygen demand is possible in 2D wave-mixed SU bioreactors, which is a limitation of the 1D-motion rocker-type bag bioreactors. Nevertheless, it should be emphasized, that animal and human cell cultures with low oxygen demands do not require such high oxygen transfer rates (see also Sect. 14.5) and that the maximum power inputs may cause cell damage to shear sensitive cells.

An even more complex motion is performed by the XRS 20 Bioreactor System, which consists of a 3D culture bag with integrated optical SU sensors for pH and DO measurement, offering a maximum working volume of 20 L. The system uses a simultaneous bi-axial rocking motion (3D) and is designed to give the flow a tumbling characteristic. According to the manufacturer, this results in almost three-times lower mixing times ($t_m < 20$ s) than the aforementioned 1D rockers (50–98 s) at comparable maximum rocking rates of about 40 rpm. Consequently, the k_La values that can be achieved are also higher. For example, $73\ h^{-1}$ is claimed for 40 rpm and 15° on both axes (www.pall.com), however, no data can be found in the scientific literature.

14.3.2 Stirred Rigid Systems

Due to their free-standing, rigid plastic vessels, these liter scale systems (Mobius® CellReady bioreactor, UniVessel® SU bioreactor, BioBLU, CellVessel) do not require an outer support container. Furthermore, folding stress, which is likely to occur in the plastic films of bag systems and may cause film layers to break, thus leading to leaks under internal pressure from the medium, is eliminated (Gossain et al. 2010). The first stirred SU bioreactor with a rigid cultivation container was the Mobius® CellReady bioreactor (Merck Millipore). The cultivation container, with a total volume of 3 L, provides a maximum working volume of 2.4 L and a recommended minimum volume of 1.0 L (for geometrical details see Table 14.3). The bioreactor is equipped with a single marine impeller and can be aerated by open pipe and micro spargers (sintered polyethylene, 15–30 µm nominal pore size). Measuring DO and pH values is performed by electrochemical probes, which have to be pre-sterilized before being introduced into the bioreactor vessel via 12 mm screw ports in the vessel lid. This increases the risk of contaminations and requires sensor polarization and calibration prior to use. Temperature is monitored with a non-invasive Pt-100 probe that is inserted into a plastic sleeve and controlled via heating blankets.

Due to the small bubbles produced by the microsparger, k_La values of up to 35 h^{-1} can be achieved at aeration rates of 0.25 vvm and impeller speeds of 250 rpm, which corresponds to tip speeds of 1.0 $m \cdot s^{-1}$ (Kaiser et al. 2011b). The authors defined the correlation for the k_La (in h^{-1}) given in Eq. 14.9 as a function of the aeration rate Q_F (in vvm) and the impeller tip speed u_{tip} (in $m \cdot s^{-1}$).

$$k_La = 4.249 - 10.61 \cdot u_{tip} + 60.0 \cdot Q_G + 4.606 \cdot {u_{tip}}^2 - 161.7 \cdot {Q_G}^2 + 160.4 \cdot u_{tip} \cdot Q_G \quad (14.9)$$

Using the decolorization method, mixing times in the Mobius® CellReady of between 55 and 7 s were determined for a 2.0 L working volume and tip speeds of 0.2 and 1.0 $m \cdot s^{-1}$, respectively. Due to the low amount of mixing in the upper part of the vessel resulting from the single bottom-mounted impeller, the mixing time increased significantly as the filling volume increased. Mixing times (at $u_{tip} = 0.2\ m \cdot s^{-1}$) of up to 78.6 s were determined for a 2.5 L working volume (Kaiser et al. 2011b). Good correlation of the mixing time (in s) with the specific power input P/V (in W m^{-3}) was established according to Eq. 14.10. It should be noted that the exponent is similar to the third radical, which can be derived theoretically, assuming fully-turbulent conditions (see Sect. 14.5).

$$t_{m,95\%} = 26.54 \cdot (P/V)^{-0.36} \quad (14.10)$$

At tip speeds of up to 2 $m \cdot s^{-1}$, the specific power input of the marine impeller at the maximum working volume was about 187 $W \cdot m^{-3}$, based on a numerically predicted power number Ne of 0.3 (see Sect. 14.5), and was confirmed by torque

Table 14.3 Summary of geometrical details of commercially available stirred SU bioreactors with cylindrical vessels

Bioreactor	Total volume V_T (L^3)	Min./max. liquid volume V_L (L)	Vessel diameter D (mm)	Impeller diameter d (mm)	Geometric ratios (−) H/D^a	H_L/H^b	d/D^c
BIOSTAT® UniVessel 2 L SU	2.6	0.6/2.0	126[d]	55	1.92	0.74	0.44
BIOSTAT® CultiBag STR	68	12.5/50	370	143	1.80	0.72	0.39
	280	50/200	585	225	1.80	0.74	0.38
	700	125/500	815	310	1.80	0.69	0.38
	1,300	250/1,000	997	379	1.81	0.76	0.38
Mobius® CellReady	3	1.0/2.4	137	76	1.82	0.80	0.55
	60	10/50	340	109	2.10	0.80	0.32
	250	40/200	540	183	2.10	0.69	0.34
CelliGEN® BLU	5	1.25/3.75	170	100	1.50	0.75	0.59
	14	3.5/10.5	214	100	2.00	0.75	0.47
	50	18/40	337	160	1.70	0.80	0.47
S.U.B. (Hyclone)	65.5	25/50	349	118	2.29	0.65	0.34
	120	50/100	438	146	2.18	0.87	0.33
	316	125/250	597	200	1.94	0.79	0.34
	660	250/500	756	251	1.93	0.78	0.33
	1,320	500/1,000	959	321	2.09	0.71	0.33
	2,575	1,000/2,000	1,194	398	1.93	0.78	0.33
XDR	n.d.	4/10	200	135	1.50	0.68	0.68
	n.d.	10/50	305	203	2.50	n.d.	0.67
	260	40/200	559	203	1.50	0.77	0.36
	560	100/500	762	254	1.50	0.89	0.33
	1,100	200/1,000	965	305	1.50	0.91	0.32
	2,200	400/2,000	1,219	406	1.50	0.91	0.33

[a]Vessel height-to-diameter ratio
[b]Normalized filling height (maximum)
[c]Impeller-vessel-diameter ratio
[d]The vessel has a slope of 1.2° resulting in a top-wards increase of the vessel diameter from 122 to 130 mm. n.d. – not defined

measurements (Löffelholz et al. 2010). This power input is within the range of typical cell culture applications, as stated by Nienow (2006). However, such high impeller speeds are neither advisable, due to vortex formation in the unbaffled vessel, nor required for most cell culture applications.

Single impellers are also used in BioBLU bioreactors (Eppendorf/New Brunswick), which are agitated by 3-blade pitched blade impellers (also referred to as 'Elephant ear' impellers). These impellers induce an upwards-directed axial flow with a clockwise rotation. The impeller blades are mounted at 45° and the impeller-to-vessel diameter ratio is 0.59 in the BioBLU 5c and 0.47 in the BioBLU 14c/50c (see Table 14.3). The power number for the impellers is Ne = 1.3 (www.eppendorf.

com), which is comparable to its conventional counterpart. Zhu et al. (2009) reported a power number of Ne = 1.7 in a baffled glass vessel (d/D = 0.45). Similar to the Mobius® CellReady 3 L bioreactor, a porous microsparger (7–12 μm pore size) is used for aeration and, therefore, comparable k_La values can be assumed at comparable specific power inputs. However, no data are available in the scientific literature.

Small scale versions of the BioBLU bioreactor, called BioBLU 0.3c, can be used in combination with a DASbox (DASGIP), representing a stackable modular system with up to 32 or more parallel cultivation vessels. The cultivation containers provide working volumes of 100–250 mL (www.dasgip.com) and are, therefore, suitable for screening experiments and process development, allowing DoE approaches and QbD compliant proceedings. Agitation is performed using magnetically-coupled top-driven 3-blade 45° pitched blade impellers that are geometrically similar to the impellers in the L-scale BioBLU bioreactors. The process critical parameters (i.e. DO, pH and optical density) are measured by optical sensors, following industry standards. Integrated dip tubes enable media addition, sampling and aeration. A special feature of the DASbox system is the liquid-free Peltier element, which controls the temperature and condensation in the exhaust air. This can be used to reduce volume loss through evaporation, which is particularly important in small scale bioreactors, where volume change may affect the process. A case study describes the successful expansion of human pluripotent stems cells, where cell yields of up to $2.3 \cdot 10^6$ cells $\cdot$ mL^{-1} were obtained in a 7-day culture (Olmer et al. 2013).

The rigid UniVessel® SU bioreactor (Sartorius Stedim Biotech) is the first commercially available rigid SU cell culture bioreactor agitated by two-stage impellers. The three elements of the segment blade impeller (SBI) are similar in shape to the 'Elephant ear' impellers of the BioBLU, but they have a lower blade angle of 30°, which results in lower power inputs. The power number above the critical Reynolds number that is required to achieve fully turbulent conditions ($Re_{crit} \approx 2 \cdot 10^4$) was determined by CFD to be Ne = 1.5, which was also confirmed by torque measurements (Löffelholz 2013). The impellers have a diameter of 54 mm and the lower one is positioned at a distance of 47 mm ($h_R/D = 0.39$) from the bottom of the vessel. The impeller distance is 70 mm ($c_s/d_R = 1.3$), which enables the individual impellers to form individual flow regions without significant interactions between the impeller discharges (Liepe et al. 1998). This was confirmed by our own CFD fluid flow analysis and predicted power inputs (data unpublished). Because of the manufacturing process, the diameter of the cylindrical vessel (D) increases towards the top (from 122 to 130 mm), but the mean vessel diameter results in a common impeller-to-vessel diameter ratio of 0.43 (see Table 14.3). Aeration is performed by a submerged L-shaped macro-sparger with small holes (0.5 mm, 14 holes) and/or via the headspace.

Comprehensive engineering characterizations of the UniVessel® SU bioreactor have been carried out in several studies (Kaiser et al. 2011a; Löffelholz et al. 2013a, b; Jossen et al. 2014). CFD simulations where the steady-state flow was predicted using an approach based on Reynolds averaged Navier-Stokes (RANS) equations

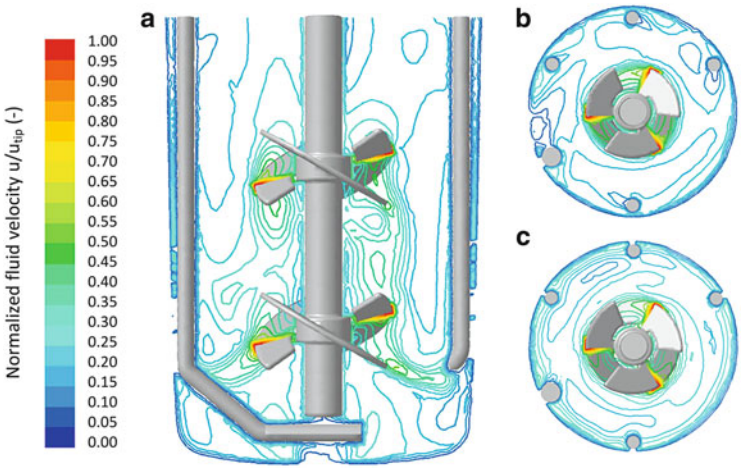

Fig. 14.4 CFD results for flow prediction in the UniVessel® SU. The fluid velocities are normalized by the impeller tip speed u_{tip}. For improved clarity the probes and part of the harvest tube are not shown. (**a**) *Front* view; (**b**) *Top* view, *upper* impeller mid-plane; (**c**) *Top* view, *lower* impeller mid-plane

with a multiple-reference-frame methodology were validated by Particle Image velocimetry (PIV) measurements, which confirmed the expected axial flow pattern of downward pumping discharges from the clockwise rotating SBIs (see Fig. 14.4). Not entirely surprisingly, the maximum fluid velocities predicted at the tips of the impellers agreed well with theoretical tip speeds (see Eq. 14.21). Considerably lower velocities ($v \leq 0.1\ u_{tip}$) were predicted near the vessel bottom, in particular below the impeller shaft, and in the upper portion of the vessel, although the effect of high filling levels was less pronounced than in the Mobius® CellReady because of the upper SBI. The discharge from the lower impeller was inclined towards the vessel wall, resulting in a separate flow loop with low axial fluid velocities near the bottom. This effect could be explained by the relative low impeller blade angle (30°) and the high off-bottom clearance ($h_R/d = 0.41$) (Jossen et al. 2014). Comparing the fluid flow pattern with the BIOSTAT® CultiBag STR pilot scale models, it was possible to establish good qualitative and quantitative agreement, indicating the scalability of the benchtop bioreactor (Kaiser et al. 2011a).

The primary and secondary axial flow numbers defined by Eqs. 14.11 and 14.12, which represent dimensionless volume flow rates through the impeller's cross-section and can be used to estimate the circulation time within bioreactors (Liepe et al. 1998), were predicted to be 0.4 and 0.77 respectively. These values are within the range of conventional stirrers, for which primary flow numbers between 0.17 and 1.27 have been reported (Patwardhan and Joshi 1999; Patwardhan 2001; Kumaresan and Joshi 2006; Ayranci et al. 2012). Furthermore, a primary flow number of 0.7 for the 'Elephant ear' impeller was obtained in a baffled tank, where the axial flow is enhanced by the lower tangential circulation (Zhu et al. 2009).

$$Fl_{z,p} = \frac{2 \cdot \pi}{N_R \cdot {d_R}^3} \cdot \int_{r=0}^{r=d_R/2} r \cdot v_z(r)\ dr \tag{14.11}$$

$$Fl_{z,s} = \frac{2 \cdot \pi}{N_R \cdot {d_R}^3} \cdot \int_{r=0}^{r=R_r} r \cdot v_z(r)\ dr \tag{14.12}$$

Similar to the Mobius® CellReady 3 L bioreactor, the mixing times in the UniVessel® SU bioreactor were found to be in a range of between 2 and 40 s, depending on the power input and filling volume ($< 250\ \mathrm{W \cdot m^{-3}}$; > 1 L). Again the slopes of the regression functions of t_m against P/V (i.e. -0.3) (Kaiser et al. 2011a; Löffelholz et al. 2013b) were close to theoretical values valid for turbulent conditions where

$$c_H = t_{m,95\%} \cdot N_R = const. \tag{14.13}$$

with c_H representing the dimensionless mixing number that defines the number of stirrer rotations required to achieve the desired homogeneity. In the case of the UniVessel® SU bioreactor a mixing number of $c_H = 18$ was predicted, which indicates that agitation is in the performance range of conventional impellers, as reported by Liepe et al. (1998).

To characterize the gas distribution and the oxygen mass transfer inside the UniVessel® SU bioreactor, CFD multiphase simulations with an Euler-Euler extended RANS approach were performed (Kaiser et al. 2011a; Löffelholz 2013) and the k_La values for a wide range of operating conditions were determined using the conventional gassing-out method (Löffelholz 2013). For the low gassing rates typically used in cell culture applications, no profound effect on the shape of the flow pattern could be identified (Kaiser et al. 2011a), which agreed qualitatively with findings of Zhu et al. (2009). However, the rising gas lowers the velocities of the downward directed fluid flow, which was also found in previous studies with conventional cell culture bioreactors (Kaiser 2009). The bubble flow around the impeller shaft resulted in lower fluid velocities and momentum exchange between the pair of impellers, and two-phase flow. Surprisingly, the gassed power input $(P/V)_g$ was found to be higher than for ungassed conditions (P/V). This is in contrast to expectations and measurements realized for the 'Elephant ear' impeller by Zhu et al. (2009), who found that $(P/V)_g$ decreased by up to ≈ 30 % when the impeller was in down-pumping mode. Nevertheless, it should be noted, that the CFD predicted power number in the UniVessel® SU also decreased (by ≈ 30 %) when critical gas flow rates were exceeded (e.g. 0.5 vvm), which may be explained by low gas dispersion (i.e. impeller flooding).

The experimentally determined k_La values for the UniVessel® SU (in $\mathrm{h^{-1}}$) could be correlated by Eq. 14.14, using the specific power input (in $\mathrm{W \cdot m^{-3}}$) and the superficial gas velocity (in $\mathrm{m \cdot s^{-1}}$). The strong influence of the superficial gas velocity is again indicated. For example, the k_La value was, depending on the

specific power input ($0.4\ \mathrm{W \cdot m^{-3}} < P/V < 150\ \mathrm{W \cdot m^{-3}}$), in the range of 10–50 $\mathrm{h^{-1}}$ for 0.01 vvm ($v_G = 2.8 \cdot 10^{-4}\ \mathrm{m \cdot s^{-1}}$) and 20–83 $\mathrm{h^{-1}}$ for 0.02 vvm ($v_G = 5.7 \cdot 10^{-4}\ \mathrm{m \cdot s^{-1}}$).

$$k_L a = 7.97 \cdot 10^3 \cdot (P/V)^{0.25} \cdot {v_G}^{0.87} \tag{14.14}$$

Other customized, rigid, L-scale SU stirred bioreactors with single or multi-stage impellers are available from Creel (Denmark). The cultivation containers have internal diameters and heights of up to 120 and 630 mm, depending on the desired total working volume. For mL scale applications the ambr 250 bioreactor (TAP biosystems) can be used. The baffled bioreactor vessels, which are equipped with two Rushton turbines, mimic classic bioreactors and, therefore, may provide good scale-down models for screening experiments. However, no engineering data have been published at the time of writing.

14.3.3 Stirred Bag Systems

In contrast to the rigid systems, stirred bag SU bioreactors require a support container to fix and shape the cultivation bag. This can either be heated electrically by heating blankets or can incorporate water-filled double jackets for temperature control. The cultivation bags need to fit perfectly into their holding devices for optimum performance, in particular with regard to heat transfer (Weber et al. 2013). Thus, cavities, pockets and folds, which can be attributed to the bag unfolding during installation, need to be prevented.

In 2006, the Thermo Scientific Single Use Bioreactor (S.U.B.), which was developed as a result of cooperation between Hyclone and Baxter (Eibl and Eibl 2011), was the first large-scale SU stirred bag bioreactor before Xcellerex launched its XDR SU stirred-tank bioreactor. Both systems are agitated by pitched axial flow impellers that are mounted off-center, eliminating the fluid vortex that is often observed in unbaffled vessels. Thus, no baffles are required in these SU stirred bioreactors. The Xcellerex bioreactor has a magnetically coupled, bottom-driven impeller, whereas the HyClone system is top-driven (Shukla et al. 2012).

The Xcellerex's XDR product family includes scales from 50 to 2,000 L and was recently extended by the XDR-10, which can handle volumes from 4.5 to 10 L (see Table 14.3). Unfortunately, only limited engineering data are available and none of them have been published in the scientific literature. According to the manufacturer, $k_L a$ values of up to 9.5 $\mathrm{h^{-1}}$ are achievable in the XDR-1000 using a specific (ungassed) power input of 5.8 $\mathrm{W \cdot m^{-3}}$ and an air flow rate of 15 $\mathrm{L \cdot min^{-1}}$ (single sparger configuration). It should be noted that, under those aeration rates, the specific power input by aeration is about 3 $\mathrm{W \cdot m^{-3}}$, assuming isothermal gas expansion.

More comprehensive characterizations of the S.U.B. Hyclone bioreactors (50 and 250 L scale) have been carried out in our own laboratories (Ries 2008; Löffelholz et al. 2010; Löffelholz 2013). CFD models for the S.U.B. 50 L, which were validated by PIV measurements (Löffelholz 2013), revealed that the pitched blade impeller generated a downward pumping axial flow pattern, where the fluid recirculated upwards along the outer walls. Below the impeller, two differently-sized flow loops are induced due to the off-center position of the impeller (Löffelholz 2013a; Löffelholz et al. 2013a). Based on the steady fluid flow pattern, a constant power number of $Ne = 1.9$ was predicted above a critical Reynolds number of $4 \cdot 10^4$ (Löffelholz et al. 2010). This gives CFD predicted specific power inputs of up to 19 $W \cdot m^{-3}$ at 50 L (with a tip speed of 3.1 $m \cdot s^{-1}$), which is about 20 % lower than the experimentally measured 24 $W \cdot m^{-3}$ (Löffelholz 2013). Reported mixing times (9–155 s) and k_La values (2–25 h^{-1}) for typical cell culture conditions are comparable to conventional and other SU stirred bioreactors at pilot scale (see below) (Ries 2008; Löffelholz et al. 2010).

Other stirred bag bioreactors are the Mobius® CellReady 50 and 200, which are agitated by bottom-mounted impellers with four blades pitched at 13°. Power numbers were determined to be $Ne = 3.2$ (50 L) and $Ne = 4.0$ (200 L), which results in specific power inputs of up to 120 $W \cdot m^{-3}$ (50 L) and 33 $W \cdot m^{-3}$ (200 L) at maximum tip speeds of 1.7 and 1.1 $m \cdot s^{-1}$ respectively. Although the impellers are mounted off-center, a single, top-mounted baffle is integrated into the bag in order to prevent vortex formation. In contrast to the Hyclone and XDR bags, the Mobius® systems have a round, rigid vessel base, which is intended to make installation easier and prevent folds in the bag.

The mixing times of the 50-L and 200-L Mobius® CellReady bioreactor were measured using conductivity probe responses at four locations (top, middle, bottom, and inside the Mobius® SensorReady loop) after adding a tracer (Dekarski 2013). Depending on the power input ($\approx$ 1.5 to 30 $W \cdot m^{-3}$) average mixing times in the range of 25 and 38 s were determined at maximum filling levels. The measured k_La values at the 50 L scale were in the range of 4 and 49 h^{-1}, using power inputs of up to 10 $W \cdot m^{-3}$ and aeration rates of between 0.0025 and 0.05 vvm. At the 200 L scale, slightly higher k_La values of up to 60 h^{-1} have been reported (Dekarski 2013), but the required power input was also higher (36 $W \cdot m^{-3}$). Surprisingly, a further increase in power input (to 51 $W \cdot m^{-3}$) did not result in higher mass transfer rates.

In contrast to the aforementioned stirred SU bag bioreactors, the BIOSTAT® CultiBag STR family (Sartorius Stedim Biotech), which offer working volumes up to 2,000 L, are agitated by two impellers mounted at a distance of $c/d_R \approx 1.3$ on the centered shaft (Noack et al. 2010). Two impeller configurations are available: two three-bladed segment impellers (SBI-SBI) and a combination with a lower-mounted six-blade Rushton turbine (disk impeller, SBI-RT). The latter is known to improve gas dispersion (Liepe et al. 1998; Zlokarnik 1999; Noack et al. 2010). The cultivation bags, which are designed very close to conventional stainless steel bioreactors in terms of vessel geometry, agitation and aeration (Weber et al. 2013), have a convex shaped bottom and have height/diameter ratios of about 1.8:1

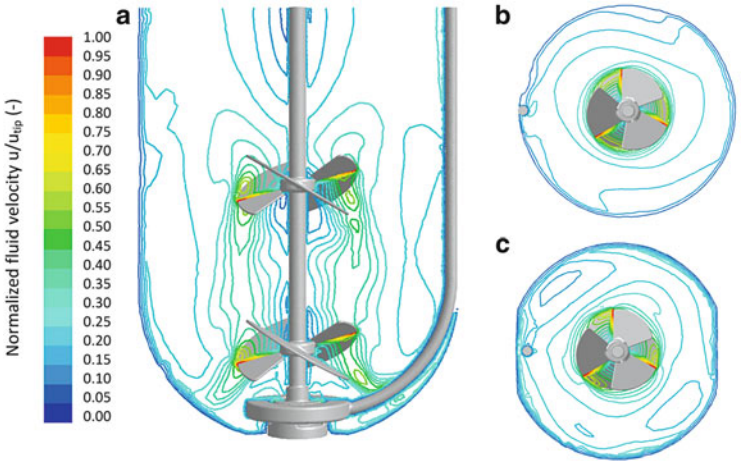

Fig. 14.5 CFD results for flow prediction in the BIOSTAT® CultiBag STR 50 L. The fluid velocities are normalized by the impeller tip speed u_{tip}. (**a**) *Front* view; (**b**) *Top* view, *upper* impeller mid-plane; (**c**) *Top* view, *lower* impeller mid-plane

(see Table 14.3). Furthermore, the impeller/vessel diameter ratio is 0.38 and the normalized off-bottom clearance *hR*/*D* of the lower impeller is 0.24, which are both within typical ranges for cell culture applications. The cultivation bags are aerated by either a classic ring sparger with 0.8 mm holes or a microsparger with 0.15 mm holes.

Comprehensive engineering characterization was carried out for fluid flow, power input, mixing times, oxygen mass transfer and microcarrier suspension at scales of up to 2,000 L for both animal and human cell cultures (Kaiser et al. 2011a; Löffelholz 2013; Löffelholz et al. 2013a, b; Jossen et al. 2014). CFD simulations, which were verified by PIV measurements, revealed the expected axial flow pattern for the impeller configuration with two SBI's, underlining the good scalability from the UniVessel® 2 L SU (see Fig. 14.5; compare Sect. 14.5). The highest fluid velocities were predicted at the blade tips and correlated well to the theoretical tip speeds ($u_{tip} = \pi \cdot d_R \cdot N_R$) for both impeller configurations. The fluid velocities decreased along the impeller discharge, whereas relative velocities ranging between 0.03 and 0.15 u_{tip} were predicted in the bulk region. Interestingly, relatively strong radial inclination of the impeller discharges of both the upper and the lower SBI were predicted, which resulted in two comparably sized flow loops. As already reported for conventional stirred vessels (Alcamo et al. 2005), the jet of the RT in the SBI-RT configuration showed a slight downward inclination, which can be explained by the absence of baffles. Nevertheless, the main body of the radial discharge from the lower RT was pumped towards the outer wall, where it impinges on the outer wall, splits, and moves up and down, forming two recirculating loops. Due to the low bottom clearance and the round-shaped bottom, the lower loop is significantly smaller than the upper. The latter reaches the liquid surface resulting in

extensive mixing of the vessel contents, while a less pronounced swirl along the bottom wall was found. In both configurations, the interaction of the two impellers can be ignored due to the high cS/dR ratio, which was confirmed by PIV and power input measurements (Löffelholz 2013).

The power input was predicted by CFD and experimentally determined by stirrer torque measurements for both ungassed and gassed conditions (Löffelholz 2013). The total power input (P/V) is usually applied to make a comparison or to scale up bioreactors, even though the effect of aeration is normally negligible, due to the low gassing rates used for mammalian cell cultures (Nienow 2006; Garcia-Ochoa and Gomez 2009). For ungassed conditions, maximum specific power inputs of approximately 86 and 240 $W \cdot m^{-3}$ were achieved at a tip speed of 1.8 $m \cdot s^{-1}$ for the SBI-SBI configuration and the SBI-RT configuration in the BIOSTAT® CultiBag STR 50 L, respectively. In contrast to expectations, an increase in the power input of 15 % was reported for an aeration rate of 0.02 vvm. Only minor differences in CFD-predicted power numbers were found for the different scales of the BIOSTAT® CultiBag STR. This can be explained by minor differences in the geometric ratios of the various size vessels and numerical uncertainties at larger scales. Power numbers of between $Ne = 1.1$ (SBI-SBI, 50 L) and $Ne = 3.1$ (SBI-RT, 50 L) were obtained. Using a tip speed of 1.8 $m \cdot s^{-1}$, power inputs of up to 48 $W \cdot m^{-3}$ (SBI-SBI) and 133 $W \cdot m^{-3}$ (SBI-RT) were achieved at the 200-L scale. This decreased even further at the 1,000-L scale to 28 $W \cdot m^{-3}$ (SBI-SBI) and 73 $W \cdot m^{-3}$ (SBI-RT).

In order to estimate potential cell damage as a result of agitation induced shear forces, mean local shear gradients were estimated. The results can be correlated by Eq. 14.15, where the P/V must be inserted in $W \cdot m^{-3}$ and the geometric parameters (d_R, D and V_L) are given in m and m^3, respectively. This equation is valid for working volumes of up to 1,000 L and, interestingly, predicted shear stresses in the Hyclone S.U.B. can also be described quite well by this correlation, even though the impeller geometry of the Hyclone S.U.B. is significantly different.

$$\dot{\gamma}_{NT} = 0.05 \cdot \left(\frac{P}{V}\right)^{1/3} \cdot \left(\frac{d_R}{D}\right)^{-2.7} \cdot V_L{}^{-0.16} \tag{14.15}$$

Depending on the scale and applied power input, shear rates between 0.1 and 30 s^{-1} were predicted in the BIOSTAT® STR bags, which corresponds to shear stresses of 10^{-4} Pa and 0.03 Pa, assuming water-like culture media (i.e. viscosity of ≈ 1 mPa · s). Significantly higher critical values (in the order of 100–300 Pa) for causing substantial cell damage have been reported (Chisti 2000). Nevertheless, physiological effects, which do not necessarily result in physical breakage of the cells, have also been observed at moderate levels of stress in the range of 0.5–5 Pa (corresponding to 500–5,000 s^{-1} in water-like culture broths) (Yim and Shamlou 2000). Even though maximum shear rates can be three to four orders of magnitudes higher than the volume-averages, it was stated that no cell damage is expected under typical cell culture conditions. This was confirmed by CHO cultivations,

where cell densities between 6 and $7.5 \cdot 10^6$ cells $\cdot$ mL^{-1} with viabilities above 96 % were achieved using chemically defined minimal medium (Löffelholz 2013).

Using conductivity methods and CFD predictions, mixing times ($t_{m,95\%}$) of between 10 and 60 s, depending on the power input (0.86–86 W $\cdot$ m^{-3}), were found at the maximum filling level for the 50-L bioreactor. Due to the larger liquid volume, between 20 and 60 s were measured in the 200-L scale (1.5–49 W $\cdot$ m^{-3}) (Löffelholz 2013). Therefore, it can be stated that the level of mixing is sufficient for cell culture applications, and the performance is comparable to conventional stirrers (Kaiser et al. 2011a). Similar results have been reported for oxygen mass transfer. In the BIOSTAT® CultiBag STR 50 L, a maximum k_La value of 35 h^{-1} was determined at an aeration rate of 0.1 vvm (Löffelholz et al. 2013b), indicating sufficient oxygen supply for cultures with a low to medium oxygen-demand. At these aeration rates, the mean bubble diameter determined by the Shadowgraphy technique was 5 mm. Not entirely surprisingly, detailed analysis indicated larger bubbles near the impeller shaft, while larger volume fractions of smaller bubbles ($d_{B,32} = 1$–4 mm) were observed near the vessel wall. This is an indication of the low gas dispersion capacity of the SBI impellers used in typical cell culture applications.

The Nucleo™ bioreactor and the ATMI Life Sciences' Integrity™ PadReactor™ have cube shaped bags with a paddle-shaped mixing element that rotates in an elliptical motion. From an engineering view point both systems are identical. Both the PadReactor™ and the Nulceo™ system include a 20 μm microsparger that is fixed to the mixing element, resulting in dynamic aeration (Rodriguez et al. 2010). As demonstrated in computational simulations, mixing in the Nucleo™ and PadReactor™ systems follow both radial and axial paths, while the walls of the cubical vessel act as baffles, preventing vortex formation (Farouk and Moncaubig 2011). Consequently, efficient mixing and solid suspension is achieved and microcarriers can be brought into suspension at impeller speeds as low as 30–50 rpm (tested with SoloHill collagen microcarriers, 125–212 μm) (Rodriguez et al. 2010; Patel et al. 2012).

14.3.4 Orbitally Shaken Bioreactors

The most often used orbitally shaken bioreactors include shake flasks, TubeSpin® bioreactors (Techno Plastic materials) and microwell plates. The latter provide miniaturization, which is advantageous for the processing of a large number of different cultivation experiments and for media optimization (Kensy et al. 2005).

TubeSpin® (also known as CultiFlask 50 disposable bioreactor from Sartorius Stedim Biotech) technology was initially developed in an attempt to provide 'bioreactor-equivalent' conditions for screening experiments at 50 mL scale (De Jesus et al. 2004; Werner et al. 2010a). The special centrifuge tubes with frusto-conical bottoms have ventilation caps for gas exchange with the incubator. Reported k_La values are up to 21 h^{-1} when operating at 150–240 rpm with

10–30 mL filling volume (Werner et al. 2010a). The experimental data could be correlated by Eq. 14.16, where V_L is the liquid volume (in L), N_R is the shaking frequency (in rpm) and d_0 is the shaking diameter (in mm).

$$k_L a = \left(1.196 + 4.089 \cdot 10^{-3} \cdot N_R - 80.3 \cdot V_L - 0.021 \cdot d_0 + 0.1663 \cdot N_R \cdot V_L + 1.252 \cdot 10^{-4} \cdot N_R \cdot d_0 + 0.317 \cdot V_L \cdot d_0\right)^2 \quad (14.16)$$

During the last decade, engineering parameters for various small scale systems, including power input, mixing time and oxygen mass transfer, have been widely reported (Büchs et al. 2000; Micheletti et al. 2006; Peter et al. 2006; Zhang et al. 2010; Tan et al. 2011; Wen et al. 2012). Furthermore, advanced parameters concerning shear stress and turbulent energy were predicted in single wells of microtiter plates (Zhang et al. 2008a), in TubeSpin® bioreactors (Werner et al. 2013), shake flasks (Zhang et al. 2005), and shaken bottles (Tissot et al. 2011b).

For unbaffled shake flasks, Eq. 14.17 was established to calculate the power input (Büchs et al. 2000), while Eq. 14.18 was proposed to estimate the achievable $k_L a$ for a wide range of operational conditions (Klöckner et al. 2013). In both equations, all parameters are to be inserted in SI units, as given in the symbol list.

$$P = 1.94 \cdot {V_L}^{1/3} \cdot \rho_L \cdot N^3 \cdot D^4 \cdot {\mathrm{Re}_{SR}}^{-0.2} \quad (14.17)$$

$$k_L a = 0.5 \cdot D^{2.03} \cdot N \cdot {V_L}^{-0.89} \cdot {\nu_L}^{-0.24} \cdot {D_{O_2}}^{0.5} \cdot g^{-0.13} \cdot {d_0}^{0.25} \quad (14.18)$$

A slightly different correlation was found for differently sized cylindrical, orbitally shaken bioreactors (also valid for the 200 L scale OrbShake™, see Eq. 14.19), which can be explained by the fact that the liquid motion is different (Klöckner et al. 2013). Again, all parameters must be inserted in SI units, as given in the symbol list.

$$k_L a = 1.06 \cdot 10^{-3} \cdot D^{4.3} \cdot N^{2.12} \cdot {V_L}^{-1.2} \cdot {\nu_L}^{-0.21} \cdot {D_{O_2}}^{0.12} \cdot g^{-0.51} \quad (14.19)$$

This is valid (with an accuracy of ±30 %) for operating conditions above critical circulation frequencies N_C that guarantee rotation of the liquid and can be calculated by Eq. 14.20.

$$N_C = \frac{1}{D^2} \cdot \sqrt{0.28 \cdot \ V_L \ \cdot g} \quad (14.20)$$

While the scaling-up of shake flasks is limited to about 1 L total volume, since the maximum working volume is only 20–30 % of the nominal volume, larger volume shaken systems with cylindrical- or cube-shaped culture containers have been developed (Muller et al. 2005; Stettler et al. 2010; Tissot et al. 2011a). Typical scales were up to 30 L, even though, the nominal volumes of some prototypes exceeded 1,000 L (Tissot et al. 2010). In addition, special constructions to improve

mixing and mass transfer have been tested, including helical tracks on the inner vessel wall. By driving the liquid onto these helical tracks, the gas-liquid interface is significantly increased. Compared to non-modified vessels, five to tenfold higher k_La values (up to 55 h^{-1}) were achieved, while cell growth was comparable to small scale TubeSpin® and 30 L stirred bioreactors (Zhang et al. 2008b).

Although none of these systems made it to market, they finally led to the development of the SU 200 L orbitally shaken bioreactor system (trade name OrbShake™ bioreactor) in 2009 (Hildinger et al. 2009). By eliminating the need for internal mixing and sparging devices, the bags are considered to be an economical alternative to stirred SU bioreactors. Furthermore, typical issues, such as foam formation, are avoided. The cylindrical cultivation container with a nominal volume of 330 L is equipped with pH and pO_2 sensors and operated using the bioreactor control system. Based on measurements in cylindrical containers agitated at ≈75 rpm with a shaking diameter of 10 cm, achievable k_La values at the maximum filling level are in the order of 8 h^{-1} (Zhang et al. 2009). Significantly higher values of up to 25 h^{-1} are reported for 100 L working volume (Anderlei et al. 2009). Under these conditions, mixing times are between 25 and 70 s, depending on the shaking frequency (50–70 rpm).

14.3.5 Fixed Bed Bioreactors

Almost no engineering data for mixing time, oxygen mass transfer (k_La) or power input are available for fixed bed bioreactors in the literature. The iCELLis bioreactor is based on a compact fixed-bed packed with macroporous, non-woven, medical-grade polyethylene terephthalate (PET) microfibers, which offer a large growth surface, depending on the fixed bed volume (Moncaubeig 2013). For all scales, the bed height is fixed at 10 cm, which provides linear scalability between the small scale iCELLis nano systems with cylindrical fixed beds and the production scale iCELLis systems containing a donut-shaped basket (Lehmann et al. 2013). In both systems, two carrier compaction levels with specific surface areas of about 13,320 and 20,000 $m^2 \cdot m^{-3}$ are available, resulting in a total growth surface area of up to 500 m^2 in only a 25 L fixed bed in the largest version (iCELLis 500/500; 660 m^2 announced).

The liquid inside the bioreactor is circulated by a built-in centrifugal-based flow impeller, which pumps the culture medium through the fixed bed from the bottom to the top. When flowing down the outer wall as a thin film, the intention is for the culture medium to be effectively oxygenated in a waterfall-like flow. To date, no k_La values or comparable data has been found in the literature. Due to the separation of the pumping impeller, which runs at high rotational speeds of up to 1,500 rpm, from the growth compartment, where linear velocities of only up to 0.05 $m \cdot s^{-1}$ were determined (Drugmand et al. 2013), the suitability of the iCELLis bioreactor for the growth of shear-sensitive, adherent cultures has been confirmed (Lennaertz et al. 2013).

Similar to iCELLis fixed-bed bioreactors, the BioBLU SU packed-bed bioreactor (BioBLU 5p, Eppendorf/New Brunswick) also employs internal recirculation. This is driven by a packed-bed basket impeller that incorporates Fibra-Cel disks as the cell attachment matrix. The two horizontally-positioned perforated screens holding the bed disks are extended to the walls of the bioreactor vessel and discharge ports positioned above the basket incorporate a central hollow tube. A low differential pressure at the base of the impeller tube is generated by the rotation of these discharge ports, which results in media circulation throughout the vessel.

The Fibra-Cel, which is fabricated according to cGMP guidelines, is composed of two layers of non-woven polyester and polypropylene that are sonicated together and electrostatically treated to attract cells and facilitate their attachment (Cino et al. 2003). The high porosity of the polymer mesh of around 90 % reduces intra-carrier diffusion limitations and provides efficient cell entrapment (Meuwly et al. 2006, 2007), which reduces cell attachment time. According to Cino et al. (2003), cells can attach within 15–60 min on the Fibra-Cel disks while it normally takes about 6 h for cells to attach to microcarriers (with a normal inoculum of $1 \cdot 10^6$ cells $\cdot$ mL^{-1}). The BioBLU 5p packed-bed bioreactor is available with a vessel volume of 5 L (3.5 L working volume) and is pre-loaded with 150 g of Fibra-Cel® disks, which offer a specific surface area of $119 \cdot 10^3$ m$^2 \cdot$ m^{-3} corresponding to 0.12 m^2 of effective surface area per gram of disks. A similar bioreactor concept is used in the CellTank^{TM} bioreactor (CerCell), which provides a non-woven polymer matrix with a surface area of about 3.6 m^2. The liquid is circulated by a centrifugal-type impeller.

An external medium recirculation system is employed in the AmProtein Current bioreactor (AmProtein), which consists of a wide-body culture vessel with an inverted frusto-conical bottom on an orbital shaker platform (Hui 2009; Jia et al. 2008). The bag is fabricated from EVA plastics, which is suggested to play a major role in oxygen mass transfer within the system. It has been shown that small bubbles are absorbed onto the plastic surface, significantly increasing the specific surface area for oxygen mass transfer (Jia et al. 2008). The periodic orbital movement repeatedly washes the exposed bubbles from the vessel wall, which is further enhanced by the inverted conical bottom. Although the applied operating conditions are difficult to compare, the shaking motion was found to provide higher oxygen transfer rates than bubbling air directly into the medium (Hui 2009).

14.4 Established and New Applications for Dynamic SU Bioreactors

Today, SU bioreactors dominate in processes based on continuous suspension cell lines, where the cells are the final product (e.g. seed or inoculum train, see Sect. 14.4.1) or high titer and high value products that are produced up to medium scale. The last mentioned products include monoclonal antibodies (mAbs)

(Sect. 14.4.2), viral vaccines (Sect. 14.4.3), virus-like particle (VLP) vaccines (Sect. 14.4.4), and viral vectors for gene therapies (e.g. adeno-associated virus, paramyxovirus, lentivirus) (Negrete and Kotin 2007). Commonly, wave-mixed systems are used for the cell expansion, whereas stirred bioreactors are preferred as production bioreactors for protein therapeutics.

However, production processes for vaccines are still often performed using adherent production cells lines (e.g. *African green monkey* kidney-derived *Vero cells*, *Madin-Darby Canine Kidney* cells or PBS-1 cells) (Josefsberg and Buckland 2012; Whitford and Fairbank 2011). Both stirred (Chaubard et al. 2010; George et al. 2010) and wave-mixed (Genzel et al. 2010; Magnusson et al. 2011) SU systems operated with microcarriers as well as fixed bed bioreactors with fiber carriers (Moncaubeig 2013) have proven themselves.

As shown in the following, their development involved the establishment of novel cultivation technologies, such as large-volume (Bögli et al. 2012) and high density cell banking (Tao et al. 2011) and XD process technology (Zijlstra et al. 2012). Furthermore, users became increasingly interested in perfusion technology (see Fig. 14.6) (Bonham-Carter and Shevitz 2011; Wang et al. 2012a). While the product quality is maintained or even increased, 10- to 30-fold higher cell densities and space-time yields of the products can be obtained in perfusion mode compared to fed-batch processes. For example, the same product amounts may be produced in 50 L SU perfusion bioreactors instead of using 1,000 L fed-batch systems (Langer 2011).

Finally, the successful application of wave-mixed, stirred, hollow-fiber and fixed bed SU bioreactors for the development of cell therapeutics has been demonstrated (van den Bos et al. 2014). Section 14.4.3 provides an overview of cultivations performed with primary human therapeutic cells in dynamic SU bioreactors and focuses on the expansion of human mesenchymal stem cells (hMSCs).

14.4.1 Modern Seed Train Production with Continuous Suspension Cell Lines

Wave-mixed bioreactors were originally designed as substitutes for spinner flasks for seed train production of animal and human continuous suspension cells. Although they were viewed skeptically in the beginning, wave-mixed bioreactors are today well-established in seed train production. As shown in Fig. 14.7, pre-cultures are commonly cultivated in shake flasks, which are inoculated from pooled cells originating from the vial-based working cell bank (WCB). Detailed descriptions of seed train production with recombinant CHO cells growing in a 10 L cultivation bag (max. working volume 5 L) to produce the inoculum for the BIOSTAT® CultiBag RM 20 are provided elsewhere (Eibl et al. 2014a). Starting with the thawing of the cells and the inoculation of the shake flasks, only 8 days are

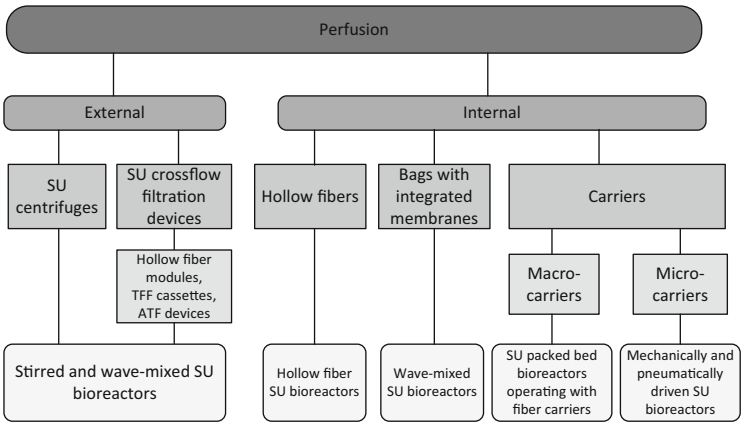

Fig. 14.6 Schematic of principal techniques applied to run SU bioreactors and devices in perfusion mode. In addition to internal perfusion (where the cells are bound on capillary fibers, membranes or microcarriers within the SU bioreactor) there is a growing interest in external perfusion. In the case of external perfusion, the cells are retained by using external SU cross flow filtration devices (e.g. Refine Technology's ATF system) or SU centrifuges (e.g. Carr UniFuge from Carr Centritech Separation Systems). If complete cell retention occurs in perfusion mode it is sensible to remove 10–20 % additional medium in order to prevent aging of the cell population. *TFF* tangential flow filtration, *ATF* alternating tangential flow

typically required to achieve medium cell densities of approximately $5 \cdot 10^6$ cells $\cdot$ mL^{-1} in the cultivation bag.

If the WCB is established using larger volumes in cryogenic bags instead of vials (Heidemann et al. 2002; Bögli et al. 2012) or using very high cell densities of approximately $1 \cdot 10^8$ cells $\cdot$ mL^{-1} in traditional vials (Alahari 2009; Tao et al. 2011), the intermediate step of shake flak expansion can be omitted. The cells of both large volume and high cell density WCBs can be generated by continuous perfusion processes in wave-mixed bioreactors (1 L working volume). Special perfusion bags with integrated, fixed or floating micro filtration membranes (see also Sect. 14.3.1) are commercially available and easy to operate (see also Fig. 14.6). By shortening the seed train production, the upstream processing of the antibody production process shown in Fig. 14.7 can be made more efficient. For example, Bögli et al. (2012) reported that it is possible to inoculate 50 L medium with a total of $5.5 \cdot 10^{10}$ with cabbage looper cells (*Trichioplusia ni; Hi-5*) after 5 days. Normally, this takes at least 10 days. The suspension cells, stored in a 120 mL cryogenic bag at −196 °C, were previously expanded in a BIOSTAT® CultiBag RM (10 L total volume) operated in repeated fed-batch mode.

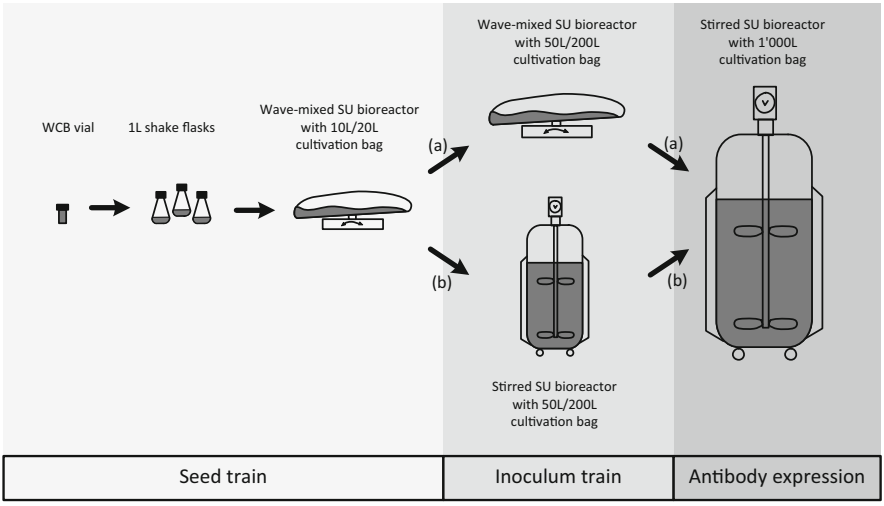

Fig. 14.7 Typical seed inoculum production and antibody expression carried out in SU bioreactors of up to 1 m^3 production scale. For the inoculum train production the user can choose between a wave-mixed and a stirred SU bioreactor system. Due to the predominance of stirred SU bioreactors in product expressions, many users switch from wave-mixed benchtop systems to stirred SU bioreactors to deliver the inoculum for the production bioreactor

14.4.2 CHO Cell-Based Production of Monoclonal Antibodies (mAbs) up to Medium Volume Scale

The great demand for therapeutic mAbs and the advantages of SU bioreactors, as described in Sect. 14.1, explain their broad usage in preclinical and clinical production processes. Meanwhile, SU bioreactors are used by many contract manufacturing organizations (CMOs) due to their scalability up to working volumes of 2,000 L. This development is supported by identical results from several comparison studies with respect to living cell density, viability profiles, expression profiles and product quality when compared to standard stainless steel vessels (Cameau et al. 2010; Diekmann et al. 2011; Smelko et al. 2011).

Continuous cell lines preferred for mAb production are nowadays genetically stable and include CHO cells, lymphoma (NS0, SP2/0) cells, human embryogenic kidney cells (HEK293), hybridomas and human embryonic retinoblast derived Per.C6 cells (Ho et al. 2013). Antibody production, which is generally carried out in fed batch mode (e.g. cells are supplemented with a concentrated nutrient solution) by using serum-/protein-free or chemically defined culture media, is often enhanced by temperature shifts (to between 28 °C and 31 °C). After 8–21 days of cultivation, the product is harvested batch wise, which leads to typical antibody titers of between 2 and 5 $g \cdot L^{-1}$ (Yang and Liu 2013).

To further increase the space-time yield of antibody production processes, SU stirred bioreactors with working volumes of up to 1 m^3 have been combined with

recently developed external SU cross flow microfiltration systems, such as the ATF module from Refine Technology. Fresh medium is continuously supplied while exhausted medium containing the product is harvested and the cells are retained inside the bioreactor. Nevertheless, the large volumes of the diluted product may complicate downstream processing.

XD technology was developed by DSM in the Netherlands in order to guarantee both high cell densities and high product titers in stirred SU bioreactors. In the case of XD technology, a cross flow filtration system is applied, which has a pore size or molecular weight cut-off that is two- to threefold smaller than the target product. Hence, not only the cells but also the product is retained in the bioreactor, which makes antibody concentrations of between 10 and 27 $g \cdot L^{-1}$ at cell densities of 10^8 cells $\cdot mL^{-1}$ realistic (Zouwenga et al. 2010).

14.4.3 Viral Vaccine and Virus-Like Particle Production

Production processes for viral human and animal vaccines differ from those of antibodies, since the production expression of viral vaccines is mostly lytic. The non-infected WCB cells are infected at the end of the growth phase by the amplified virus stock from the working virus bank (WVB). The viruses are replicated inside the cells, which leads to an increase in the cell diameter. The released viruses are processed into solutions for injections containing live (attenuated) or inactivated viruses. Because clinical doses of viral vaccines are typically smaller than those of mAbs, the production scale (100–2,500 L) is also smaller (Ball et al. 2009). However, many virus production processes require higher biosafety demands (often biosafety level 3 environments). As already mentioned, the use of animal products and in particular serum in the commercial production of viral vaccines is still relevant (Whitford and Fairbank 2011). Furthermore, there are more adherently cultivated production cell lines than in antibody production processes, including the *African green monkey* kidney-derived *Vero cells*, *Madin-Darby Canine Kidney* (MDCK) cells or C*hick Embryo Fibroblast* (CEF) cells (Chaubard et al. 2010; Hu et al. 2008). Therefore, bioreactors are used which allow 2D cell growth, such as roller bottles and multitray systems, or which operate with hollow fibers (Hirschel 2011) or microcarriers (Moncaubeig 2013). Many vaccine producers (e.g. GSK, IDT Biologica, MedImmune, Sanofi-Aventis, Virbac) have replaced roller bottles and multitray systems with microcarrier based (see overview about common microcarrier types given by Whitford and Fairbank (2011)) wave-mixed (Sect. 14.3.1) and stirred (Sects. 14.3.2 and 14.3.3) SU bioreactors. Different studies, where MDCK and Vero cells were grown on microcarriers, revealed that tenfold higher cell densities and virus titers can easily be achieved when using wave-mixed and stirred bioreactors for virus production (e.g. Influenza, Polio, mink enteritis virus) (Genzel et al. 2004, 2006; Hundt et al. 2007; George et al. 2010; Schouwenberg et al. 2010; Thomassen et al. 2012).

As an alternative to stirred and wave-mixed SU bioreactors operating with microcarriers, SU fixed bed bioreactors (Sect. 14.3.5) are used for viral vaccine production. Moncaubeig (2013) described two virus production processes based on Vero cells in an iCELLis^{TM} system (0.53, 1, 13.2, 132, 660 m^2 fixed bed made of medical-grade polyester microfibers). Moreover, scale-up from the smallest to 660 m^2 fixed bed (prototype, no yet commercially available) was successful for a human vaccine production process. The cell growth and virus productivity were equivalent to those found in a reusable, stirred 600 L bioreactor with 6 $g \cdot L^{-1}$ Cytodex microcarriers. Using an iCELLis^{TM} with 2.7 m^2 fixed bed and serum free medium, up to 11-fold higher productivity of paramyxovirus was achieved compared to T-flasks. Comparability of the small-scale iCELLis^{TM} nano bioreactor (0.53 m^2, 40 mL fixed-bed) with a CellSTACK® for the production of recombinant adeno-associated viruses was also proven by Lennaertz et al. (2013). Maximum viral yields of up to $4.5 \cdot 10^8$ vector particles per $\cdot\, cm^2$ were achieved using HEK cells. Peak cell densities of $40 \cdot 10^6$ cells $\cdot\, mL^{-1}$ were achieved with Vero cells producing an undisclosed enveloped virus in serum-free conditions in a 500 mL iCELLis^{TM} fixed-bed bioreactor (Drugmand et al. 2009).

A benchtop scale alternative is the 5 L BioBLU SU packed-bed bioreactor (see Sect. 14.3.5). It is close in design to its re-usable counterpart, which became very popular for vaccine production at laboratory scale. For example, cell densities of up to $12.4 \cdot 10^6$ cells $\cdot\, mL^{-1}$ were achieved in a 14 day culture of the *TE Fly* retroviral vector producer cell line, resulting in a maximum titer of 10^7 viral particles $\cdot\, cm^{-3}$ (Merten et al. 2001). At the time of writing, no results from vaccine production processes executed in the SU version model have been published in scientific journals, but the general applicability in CHO based protein expression has been demonstrated (Hatton et al. 2012).

Using the AmProtein Current Perfusion bioreactor fixed bed system, a total of $3.2 \cdot 10^{10}$ MDCK cells have been measured after 6 days and influenza virus production (H_1N_1) was induced with a multiplicity of infection of 0.05. The peak virus titer of about $7.68 \cdot 10^6$ hemagglutinin units per liter, which corresponds to $7.8 \cdot 10^7$ 50 % tissue culture infectious doses per mL, was obtained 3 days post infection (Sun et al. 2013). Furthermore, analysis of the cell density at different positions suggested a stable and even distribution pattern throughout the perfusion column.

Interestingly, the importance of insect suspension cells used as production organisms for vaccines has increased during recent years (Cox 2012; de Jongh et al. 2013). This concerns lytic product expressions with the baculovirus expression vector system (BEVS), which have been characterized and optimized by several authors (Kamen et al. 1996; Schmid 1996; Palomares and Ramírez 2009; Vicente et al. 2011). Fall army worm cell lines (*Spodoptera frugiperda*; *Sf-9*) as well as the cabbage looper (*Hi-5*) and its derivatives have become well established. The main advantages of insect cell and BEVS based vaccine production processes include short process time (about 5–6 days) and the inability of BEVs to infect humans (Weber and Fussenegger 2009). Thus, a biosafety level environment 1 is sufficient for the production of VLP vaccines (since they are non-replicating and

non-pathogenic due to their complete lack of DNA or RNA, but provoke high protective immunity) using insect cells and BEVS.

With respect to the quick availability of preclinical and clinical samples for seasonal and pandemic vaccine candidates, the usage of wave-mixed and stirred SU bioreactors is advantageous (Eibl et al. 2013; Hahn 2013). Currently, upstream concepts, which are entirely based on SU devices, are being realized. Eibl et al. (2013) developed an upstream concept, which is based on the wave-mixed BIOSTAT® CultiBag RM 20/50 and provided preclinical Influenza A/H_1N_1/Puerto Rico8/34 VLPs for animal studies in the single-digit $mg \cdot L^{-1}$ range. The authors used the BIOSTAT® CultiBag RM 20/50 for (1) the production of a large volume WCB of *Sf-9* cells stored in cryogenic bags at −196 °C, (2) the generation of working seed virus at −80 °C, (3) cell expansion (bag-to-bag inoculation and repeated fed batch expansion) and (4) influenza VLP stock production at 1 and 10 L scale. Due to the omission of intermediate cultivation steps in shake flaks and the increase of the scale-up rate to > 1.5 steps, time savings of about 35 % are achievable in upstream processing (USP).

14.4.4 Expansion of Human Primary Cells for Production of Cell Therapeutics

Compared to the production of vaccines and antibodies, the production of human primary cells uses small batch production processes that still take place in serum-containing media. The final products are the therapeutically relevant cells themselves, which are injected or implanted into the patient in order to treat serious disorders (e.g. cancer, myocardial, metabolic and orthopedic disorders). A distinction is made between autologous and allogeneic transplantations.

Mostly T-cells, natural killer (NK) cells, dendritic cells and hematopoietic stem cells are used for autologous transplantations, where the donors receive their own cells after biopsy, manipulation (e.g. cell activation, genetic manipulation) and cell expansion. As described by van den Bos et al. (2014), the cell amounts required for a patient's treatment can be generated in commercially available 2D SU cultivation systems, such as gas permeable bags or planar cultures (CellFactories, CellSTACK®, HyperFlask etc.). Furthermore, different published studies have revealed that clinically relevant doses of activated T-cells (mean $1.7 \cdot 10^{10}$ T cells) and NK-cells (mean $9.8 \cdot 10^9$ NK cells) can be produced in wave-mixed SU bioreactors (Wave Bioreactor) (Tran et al. 2007; Hollyman et al. 2009; Sutlu et al. 2010).

Allogeneic transplantation is characterized by the fact that the donor and the receiver of the cells are different. For clinical allogeneic therapies, the growing interest in hMSCs is obvious (Trounson et al. 2011; van den Bos et al. 2014). This can be explained by less ethical concerns and the higher safety of the hMSCs compared to human embryonic and induced pluripotent stem cells (Wang

et al. 2012b). However, the required number of therapeutic hMSCs for a single patient (70 kg) in clinical trials is in the order of $3 \cdot 10^7$ to $5 \cdot 10^8$ cells (Rafiq et al. 2013). According to Rowley et al. (2012) and van den Bos et al. (2014), clinical indications require trillions of hMSCs per year. Due to the high cell amounts, alternatives to the aforementioned 2D SU systems are still required for allogeneic therapies. Although 3D SU systems, such as SU hollow fiber bioreactors (Quantum cell-expansion system (Kilian 2013)), or SU fixed bed bioreactors (iCELLIs (Rowley et al. 2012)), offer controllable and efficient hMSC expansion, they have limited scalability. For this reason, several research groups are working on the development of scalable platforms for the expansion of hMSCs, where they are cultivated as aggregates or on microcarriers in instrumented and automated SU bioreactors. The largest working volumes have been achieved in hMSC expansions with microcarriers (cyclical perfusion or feeding mode) when stirred and wave-mixed systems have been used. After an attachment phase without agitation, mixing should be performed under low shear stress conditions in order to prevent cell damage or loss of stem cell characteristics, to achieve viable cell densities of about $1 \cdot 10^6$ cells $\cdot$ mL^{-1}. Timmins et al. (2012) succeeded in the expansion of human placental mesenchymal stem cells in 2 L wave-mixed bioreactors (0.5 L culture volume) using CultiSpher-S microcarriers over a 7 day cultivation period. Similar expansion factors were achieved for bone marrow-derived (hBM-MSCs) and adipose tissue derived mesenchymal stem cells (hADSCs), where expansion factors of between 16 and 18 (cell densities between 1.4 and $2.5 \cdot 10^5$ cells $\cdot$ mL^{-1}) were reported for 14 days of cultivation in glass spinners (Santos et al. 2011).

In a 12-day cultivation in the stirred Mobius® CellReady 3 L bioreactor using serum-supplemented culture medium (10 %) and microcarriers, cell densities of between 2.5 and $2.7 \cdot 10^5$ hBM-MSCs $\cdot$ mL^{-1} have been achieved (Cierpka et al. 2013; Jing et al. 2013). The course of a typical cultivation of hADSCs in the Mobius® CellReady 3 L (2 L culture volume), as performed in our laboratories, is delineated in Fig. 14.8a. After 6 days of cultivation, about $5.5 \cdot 10^5$ hADSCs $\cdot$ mL^{-1} were grown. Using ProNectin-F COATED microcarriers and serum-reduced Lonza medium (5 % serum), cell growth comparable to small reference scale spinner flasks was achieved. In the stirred bag bioreactor BIOSTAT® CultiBag STR 50 L we produced a total cell quantity of $1 \cdot 10^{10}$ hADSCs in a 35 L culture volume ($2.9 \cdot 10^5$ hADSCs $\cdot$ mL^{-1}) with the same microcarrier-medium combination. This number of cells is sufficient for allogeneic therapies (20 doses of $5 \cdot 10^8$ cells) for 20 patients (Schirmaier et al. 2014).

Within the scope of a collaboration project between the Zurich University of Applied Sciences, Lonza Cologne and Sartorius Stedim Biotech, the design of the stirred BIOSTAT® UniVessel SU 2 L was optimized with respect to stem cell based microcarrier suspension, in order to guarantee homogenous microcarrier-cell-aggregates and cell amounts of up to $1 \cdot 10^9$ hADSCs at high microcarrier concentrations (≥ 8 g $\cdot$ L^{-1}) (Jossen et al. 2014). Furthermore, it has been shown that direct scale-up from spinner flasks to the pilot scale BIOSTAT® CultiBag STR 50 L is possible, based on screening experiments to establish the optimal combination for the culture medium, the microcarrier type, the operational conditions and

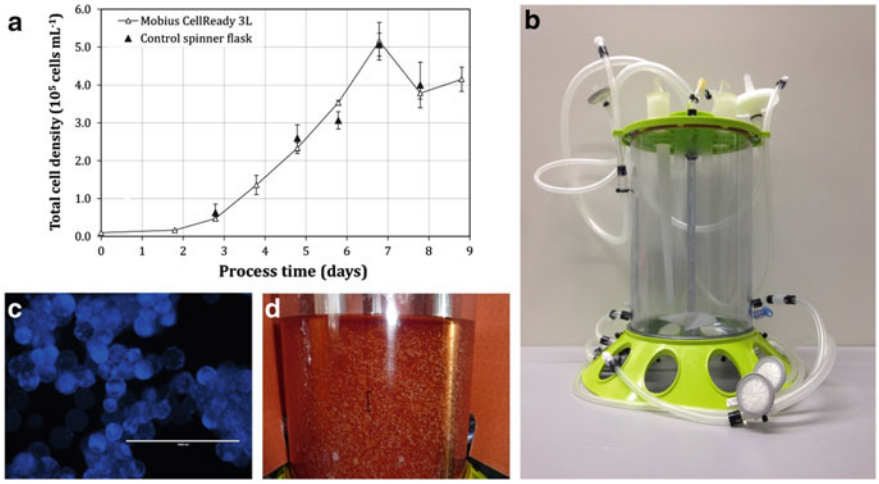

Fig. 14.8 hADSC expansion in the Mobius® CellReady 3 L (2 L culture volume). (**a**): Typical growth course (batch mode) observed in a Mobius® CellReady bioreactor compared to a control spinner flask (100 mL culture volume). (**b**): Photo of the bioreactor vessel used, which was equipped with marine impeller, microsparger and standard sensors (not shown). (**c**): DAPI colored hADSCs grown on microcarriers cultivation day 7 (metering bar = 1,000 μm). (**d**): Photo of the microcarrier-cell-suspension in the Mobius® CellReady on cultivation day 7

the most suitable engineering tools (i.e. CFD and suspension studies). Cell growth of the hBM-MSCs used was similar in the different cultivations systems (results being prepared for publishing).

14.5 Scale-Up of Processes Based on SU Bioreactors

Published case studies report the scalability of SU systems from micro- to production-scale bioreactors (Fernald et al. 2009; Legmann et al. 2009). Since scale-up principles for stirred bioreactors are generally better characterized than those for other bioreactor types, such as rocker-type wave bioreactors (Gossain et al. 2010), the main focus of this section is on stirred SU bioreactors. However, comparability with conventional bioreactors may become difficult because of factors which include eccentrically or non-vertically installed stirrers (e.g. Thermo Fisher's S.U.B., Mobius® CellReady 250), and deviation from standard impeller and sparger types used in SU bioreactors (Gossain and Mirro 2010). Not all bioreactor manufacturers meet the requirements for geometrical similarity between the scales (see Table 14.3). Nevertheless, typical height-to-diameter H/D ratios of stirred SU bioreactors are between 1:1 and 2:1, where the maximum working volume is around 70–80 % of the total volume. The impeller-to-vessel

diameter ratio is typically between 0.33 and 0.6, whereas large impellers provide efficient mixing at low impeller speeds.

The impeller diameter d_R and speed N_R determine the impeller tip speed u_{tip} defined by Eq. 14.21, which correlates well with the maximum fluid velocities and consequently the maximum shear rates within many SU bioreactors (in fact only valid for unaerated conditions) (Kaiser et al. 2011a; Löffelholz 2013).

$$u_{\mathrm{tip}} = \pi \cdot d_{\mathrm{R}} \cdot N_{\mathrm{R}} \tag{14.21}$$

Although the tip speed is often used for scaling-up in biopharmaceutical applications (Kunas and Papoutsakis 1990; Smith and Greenfield 1992; Shiragami 1997), it does not consider the actual shape of the impeller, and volume changes in fed-batch processes. Furthermore, scaling-up to larger bioreactors using a constant tip speed decreases the specific power input, as the relationship in Eq. 14.22 confirms, a relationship that was also shown for the UniVessel® SU and the BIOSTAT® CultiBag STR 50 L (Kaiser et al. 2011a).

$$P/V \propto \frac{{u_{tip}}^3}{D} \tag{14.22}$$

The most often applied scale-up approaches are based on similar specific power inputs P/V (Smith and Greenfield 1992; Al-Rubeai et al. 1995; Platas Barradas et al. 2012; Dekarski 2013), which can be predicted by Eq. 14.23 if the power number (also called Newton number, Ne) is known.

$$P/V = \frac{Ne \cdot \rho_L \cdot {N_R}^3 \cdot {d_R}^5}{V_L} \tag{14.23}$$

However, Ne is a function of the impeller type, the Reynolds number Re, the diameter ratio d/D, the bottom clearance h_R, the number of baffles etc. (Liepe et al. 1998). Reported Ne numbers for stirred SU bioreactors range from 0.3 (Mobius® CellReady, (Kaiser et al. 2011b)) to 4.2 (Mobius® CellReady). Using a constant (ungassed) specific power input as the primary scale-up criterion for three scales of the Mobius® CellReady bioreactor family (3, 50, 250 L), comparable values for cell growth (with $\mu \approx 0.0398$–$\mu \approx 0.0428\ \mathrm{h}^{-1}$), viability, and nutrient metabolism of the CHO cell line were obtained at each scale (Dekarski 2013). In addition, comparable maximum growth rates were found (0.04–0.046 h^{-1}) for *VPM8 hybridoma* cells cultivated in microwell plates and shake flasks at matched power consumptions ($\approx 40\ \mathrm{W \cdot m^{-3}}$) (Micheletti et al. 2006). This suggests that constant specific power input is, at least initially, a good basis for scale translation, even in geometrically dissimilar cultivation systems. However, it should be mentioned that almost identical growth rates (0.048 h^{-1}) and similar peak cell densities were even found in a 3.5 L stirred bioreactor in the same study, although the specific power input ($\approx 3.64\ \mathrm{W \cdot m^{-3}}$) was lower by a factor of 10 (Micheletti et al. 2006).

While no scaling-up study has been found in the literature for SU stirred systems based on mixing time, successful process transfer from the 1D rocker-type BIOSTAT® CultiBag RM to the 2D moving CELL-tainer® based on mixing time has been described for Vero cell based polio virus production (Thomassen et al. 2012). Nevertheless, based on turbulence theory, it has been suggested that mixing times in stirred systems is independent of the impeller type and inversely proportional to turbulent diffusion, as defined by Eq. 14.24:

$$t_{m,95\%} \propto \left(\frac{\varepsilon_T}{L_c{}^2}\right)^{-1/3} \tag{14.24}$$

where ε_T and L_c represent the local energy dissipation rate and the integral scale of turbulence respectively. Assuming that the integral scale is proportional to the vessel diameter, a correlation was established between mixing time and the third radical of the specific power input and the geometrical parameters (Nienow 1997):

$$t_{m,95\%} \propto \left(\frac{P}{V}\right)^{-1/3} \cdot \left(\frac{d_R}{D}\right)^{-1/3} \cdot \left(\frac{H_L}{D}\right)^{2.43} \cdot D^{2/3} \tag{14.25}$$

Löffelholz et al. (2013b) found that CFD predicted mixing times in different bioreactors from the Sartorius Stedim BIOSTAT® STR family follow the same trend (see Fig. 14.9a). However, it should be emphasized that the specific power input at larger scales increases significantly when the mixing time is kept constant during scaling-up (Junker 2004; Xing et al. 2009), which may result in unfavorable impeller speeds. Comparing different geometrically dissimilar SU bioreactors at 200 L scale (including cylindrical and cube-shaped vessels with one or two impellers), Chaubard et al. (2010) examined mixing times at constant tip speeds of between 44 and 86 s for 0.5 $m \cdot s^{-1}$ decreasing to 16 and 58 s for 1 $m \cdot s^{-1}$. In this study the BIOSTAT® CultiBag STR and the XCellerex XDR had the shortest and

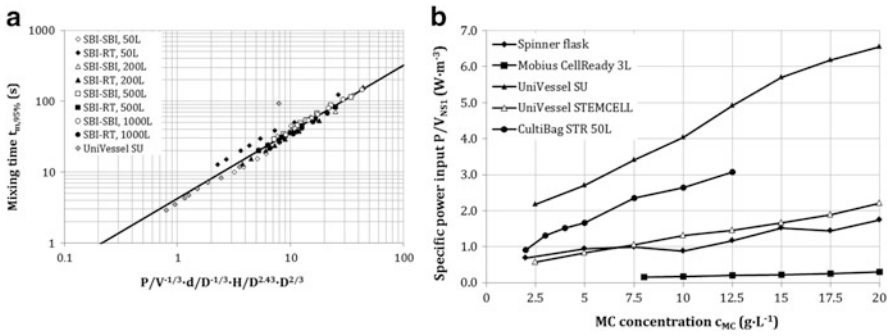

Fig. 14.9 Considerations on scale up. (**a**) Correlation of mixing times in selected stirred SU bioreactors given by Eq. 14.25 (Adopted from Löffelholz (2013)); (**b**) Specific power inputs at N_{SI} criteria for different stirred SU bioreactors

longest mixing times respectively, but there is still a lack of systematic comparisons of mixing in the SU bioreactors that consider geometrical parameters.

For microcarrier based processes, the use of mixing and suspension criteria as scale-up factors have been proposed for animal (Vorlop and Lehmann 1988; Thomassen et al. 2012) and human (Duvar et al. 1996; Hewitt et al. 2011; Kaiser et al. 2013) cells. The microcarriers have to be kept in suspension, at least for most of the batch time, if the available area is to be used effectively. The "just-fully" suspended criterion N_{S1} represents the impeller speed, where no microcarriers are located at the vessel bottom for longer than 1 s, but it does not necessarily mean that the microcarriers are homogenously dispersed throughout the bioreactor (Hewitt et al. 2011). The less common criterion N_{S1u} represents the lower limit of N_{S1}, meaning that some particles are still located on the bioreactor bottom, but none of them are at rest (Liepe et al. 1998). Although the N_{S90}, which represents the impeller speed required to lift particles up to 90 % of the filling height, is easier to determine experimentally (Zlokarnik 1999), it is not recommended for microcarrier-based processes (Kaiser et al. 2013). For several stirred SU bioreactors it was found that the N_{S1u} criterion was achieved at approximately 20 % lower impeller speeds than N_{S1} (Kaiser et al. 2013; Schirmaier et al. 2014). Typical impeller speeds for N_{S1} were between 50 and 145 rpm (corresponding to tip speeds up to 0.82 $\mathrm{m \cdot s^{-1}}$) at benchtop scales. However, between 50 and 62 rpm were required for a microcarrier suspension in the BIOSTAT® CultiBag STR 50 L. This corresponds to specific power inputs of up to ≈ 1.8 $\mathrm{W \cdot m^{-3}}$, depending on the microcarrier concentration (see Fig. 14.9b). Thus, N_{S1} and N_{S1u} are very sensitive to the vessel configuration, the agitator type and the microcarrier type used (i.e. density and size). As a result, these criteria have to be determined individually for every microcarrier-bioreactor combination.

Another typically applied scale-up criteria related to oxygen mass transfer is the specific liquid mass transfer coefficient, $k_L a$. It was, for example, used as a secondary scale-up criterion in Dekarski's study (2013) to identify suitable aeration rates at larger scales. For a given bioreactor geometry and culture medium (i.e. viscosity, density, surface tension), the $k_L a$ in stirred bioreactors is mainly influenced by the specific power input and the aeration rate (see also Eq. 14.28). The latter is quantified by either the superficial gas velocity ν_G (Eq. 14.26; for cylindrical vessels) or the volume-related gas flow rate Q_G (Eq. 14.27).

$$v_G = \frac{F_G}{A} = \frac{4 \cdot F_G}{\pi \cdot D^2} \tag{14.26}$$

$$Q_G = \frac{F_G}{V_L} \tag{14.27}$$

Obviously from Eqs. 14.26 and 14.27, the gas flow rate F_G has to be further increased at larger scales if the constant Q_G is applied ($\nu_G \propto D^{-2}$;$Q_G \propto D^{-3}$). Typical $k_L a$ values in animal cell cultures are in the range of 1 and 10 $\mathrm{h^{-1}}$ (Henzler and Kauling 1993; Langheinrich et al. 2002). For several stirred SU bioreactors the

correlation given by Eq. 14.28 can be applied, where a, b and c are empirical constants.

$$k_L a = c \cdot (P/V)^a \cdot \nu_G{}^b \tag{14.28}$$

These not only depend on the bioreactor geometry but also on the media properties (i.e. viscosity, surface tension, antifoam concentration etc.). Interestingly, the constant b (0.6–0.9) was found to be larger than a (0.25–0.45) in most SU bioreactors operated under typical cell culture conditions (e.g. Mobius® CellReady 3 L, as reported by Kaiser et al. (2011b)). This means that the influence of the gas flow rates on the $k_L a$ is more pronounced than that of the specific power input. This is in contrast to correlations obtained by van't Riet (1979) and Nienow (2006), but can be explained by the low agitation and resulting low gas dispersion of the primarily axially pumping cell culture impellers.

Nevertheless, $k_L a$ was used as a key parameter for scaling-up between geometrically dissimilar small scale (35 mL working volume) stirred and wave-mixed (2 and 3.5 L working volume) bioreactors (Hanson et al. 2009). Based on identification of achievable $k_L a$ values as a function of impeller speed and rocking rate in both systems, similar trends were observed for the DO in Immunoglobulin G producing hybridoma cultures. This implies comparable oxygen delivery rates, assuming approximately equal oxygen uptake rates, which resulted in similar culture performance based on peak viable cell density ($1.28/1.18 \cdot 10^6$ cells $\cdot$ mL^{-1}), maximum antibody concentrations (93/92 mg $\cdot$ L^{-1}) and average growth rate (0.026/0.029 h^{-1}) (Hanson et al. 2009).

Concluding Remarks

Nowadays, SU bioreactors are used by developers as well as CMOs for the production of preclinical and clinical samples. This can be explained by their high flexibility and the reduction in time and expenses if the systems are correctly implemented (Whitford 2010). Although customers can choose between several different kinds of SU bioreactors, SU stirred bioreactors operated in fed-batch mode are preferred for animal and human cell based processes. One exception is inoculum production, where wave-mixed systems have become the standard.

The broad acceptance of stirred SU bioreactors can be explained by their scalability, the similarity of their design compared to their conventional counterparts, and the availability of engineering parameters (Löffelholz et al. 2013). Furthermore, scale-up can be achieved using classical criteria, such as the specific power input (Minow et al. 2013), or by using modern technologies (Venkat and Chalmers 1996; Letellier et al. 2002), such as PIV and CFD. By performing integrated processes, such as the combination of stirred SU bioreactors with SU cross flow filtration systems, tenfold or even

(continued)

higher increases in product titers are possible. Therefore, production processes with scales between 500 and 2,000 L are regarded as sufficient.

However, three issues associated with SU bioreactors still exist: the low degree of instrumentation and automation, the lack of standardization, and the problem of leachables/extractables. Since, the cultivation vessels are only used once, SU sensors which come into direct contact with the medium are inexpensive, but do not need a long life-time (Glindkamp et al. 2010). Furthermore, sensors that are pre-configured and integrated into the cultivation system have to withstand gamma irradiation used for sterilization. Only if this is guaranteed, critical process parameters that may influence critical attributes can be determined, as required by the Process Analytical Technology initiative of the US Food and Drug Administration. Solutions for the improved standardization and reduction of leachables/extractables are under development, which will lead to further increases in the implementation of SU bioreactors in commercial GMP production processes (Langer 2012).

There are nine fields in which the future application of SU bioreactors for animal and human cell based cultivations show clear promise: (1) large-volume and high density cell banking, (2) inoculum production, (3) production of mAbs at medium-volume scales, (4) production of personalized mAbs at small-volume scale, (5) production of viral and VLP vaccines, (6) production of viral vectors for gene therapies, (7) expansion and/or differentiation of human autologous cells for cell therapeutics at small scales and (8) expansion and/or differentiation of human allogeneic cells for cell therapeutics at medium scales.

Acknowledgments The authors would like to thank M.Sc. Carmen Schirmaier and B.Sc. Valentin Jossen for the experimental work with the hADSCs in the Mobius® CellReady 3 L bioreactor and the MC suspension investigations. Gerhard Greller (Sartorius Stedim Biotech) and Mark Selker (Finesse Solutions, Inc.) we thank for the fruitful discussions.

References

Adams T, Noack U, Frick T, Greller G, Fenge C (2011) Increasing efficiency in protein supply and cell production by combining single-use bioreactor technology and perfusion. Biopharm Int Suppl 24:S4–S11

Alahari A (2009) Implementing cost reduction strategies for HuMab manufacturing processes. Bioproc Int 7(S1):48–54

Alcamo R, Micale G, Grisafi F, Brucato A, Ciofalo M (2005) Large-eddy simulation of turbulent flow in an unbaffled stirred tank driven by a Rushton turbine. Chem Eng Sci 60:2303–2316

Al-Rubeai M, Singh RP, Goldman MH, Emery AN (1995) Death mechanisms of animal cells in conditions of intensive agitation. Biotechnol Bioeng 45:463–472

Altaras GM, Eklund C, Ranucci C, Maheshwari G (2007) Quantitation of interaction of lipids with polymer surfaces in cell culture. Biotechnol Bioeng 96:999–1007

Anderlei T, Cesana C, Bürki C, De Jesus M, Kühner M, Wurm F, Lohser R (2009) Shaken bioreactors provide culture alternative. Genet Eng Biotechnol News 29:44

Aranha H (2004) Disposable systems. Bioprocess Int 2(S9):6–16

Armstrong W (1994) Polarographic oxygen electrodes and their use in plant aeration studies. Proc R Soc Edinburgh 102B:511–527

Ayranci I, Machado MB, Madej AM, Derksen JJ, Nobes DS, Kresta SM (2012) Effect of geometry on the mechanisms for off-bottom solids suspension in a stirred tank. Chem Eng Sci 79: 163–176

Ball P, Brown C, Lindström K (2009) 21st century vaccine manufacturing. Bioproc Int 7(4):18–26

Bernard F, Chevalier E, Cappia J-M, Heule M, Paust T (2009) Disposable pH sensors. Bioproc Int 7(S1):32–36

Bink L, Furey J (2010) Using in-line disposable pressure sensors to evaluate depth filter performance. Bioproc Int 8(2):44–49

Bögli NC, Ries C, Adams T, Greller G, Eibl D, Eibl R (2012) Large-scale, insect-cell-based vaccine development. Bioproc Int 10:40–49

Bonham-Carter J, Shevitz J (2011) A brief history of perfusion biomanufacturing. Bioproc Int 9: 24–31

Brecht R (2010) Disposable bioreactors: maturation into pharmaceutical glycoprotein manufacturing. Adv Biochem Eng Biotechnol 115:1–31

Büchs J, Maier U, Milbradt C, Zoels B (2000) Power consumption in shaking flasks on rotary shaking machines: I. Power consumption measurement in unbaffled flasks at low liquid viscosity. Biotechnol Bioeng 68:589–593

Cameau E, Abreu G De, Desgeorges A, Kornmann H, Charbaut E (2010) Evaluation of a single-use bioreactor for the fed-batch production of a monoclonal antibody. Biopharm Int Suppl 12–15

Chaubard J-F, Dessoy S, Ghislain Y, Gerkens P, Barbier B, Battisti R, Peeters L (2010) Disposable bioreactors for viral vaccine production: challenges and opportunities. Biopharm Int Suppl 22

Chisti Y (2000) Animal-cell damage in sparged bioreactors. Trends Biotechnol 18:420–432

Cierpka K, Elseberg CL, Niss K, Kassem M, Salzig D, Czermak P (2013) hMSC production in disposable bioreactors with regards to GMP and PAT. Chem Ing Tech 85:67–75

Cino J, Mirro R, Kedzierski S (2003) An update in the advantages of Fibra-Cel disks for cell culture. Appl Note Eppendorf

Clark KJR, Furey J (2007) Application of disposable pressure sensors to a postcentrifugation filtration process. Bioproc Int 5(S4):62–65

Cox MMJ (2012) Recombinant protein vaccines produced in insect cells. Vaccine 30:1759–1766

De Jesus MJ, Girard P, Bourgeois M, Baumgartner G, Jacko B, Amstutz H, Wurm FM (2004) TubeSpin satellites: a fast track approach for process development with animal cells using shaking technology. Biochem Eng J 17:217–223

De Jongh WA, Salgueiro S, Dyring C (2013) The use of *Drosophila* S2 cells in R&D and bioprocessing. Pharm Bioproc 1:197–213

Dekarski J (2013) Scalability of the Mobius® Cell Ready single-use bioreactor systems. Biopharm Int Suppl 26:11–17

Diekmann S, Dürr C, Herrmann A, Lindner I, Jozic D (2011) Single use bioreactors for the clinical production of monoclonal antibodies – a study to analyze the performance of a CHO cell line and the quality of the produced monoclonal antibody. BMC Proc 5(Suppl 8):P103

dos Santos F, Andrade PZ, Abecasis MM, Gimble JM, Chase LG, Campbell AM, Boucher S, Vemuri MC, da Silva CL, Cabral JMS (2011) Toward a clinical-grade expansion of mesenchymal stem cells from human sources: a microcarrier-based culture system under xeno-free conditions. Tissue Eng Part C Methods 17:1201–1210

Drugmand J-C, Esteban G, Alaoui N, Jafâr N, Havelange N, Berteau O, Castillo J (2009) On-line monitoring: animal cell cultivation in iCELLis fixed-bed reactor using dielectric measurements. In: Jenkins N, Barron N, Alves P (eds) Proceedings of the 21st annual meeting of the European Society for Animal Cell Technology. Dublin, Ireland, Springer Sciences and Business Media, pp 395–399

Drugmand J-C, Vertommen N, Knowles S, Debras F, Castillo J (2013) Linear scalability of virus production in the Integrity™ iCELLis™ disposable fixed-bed bioreactor from bench-scale to industrial scale. Appl Note

Duvar S, Müthing J, Mohr H, Lehmann J (1996) Scale up cultivation of primary human umbilical vein endothelial cells on microcarriers from spinner vessels to bioreactor fermentation. Cytotechnology 21:61–72

Eibl R, Eibl D (2009a) Disposable bioreactors in cell culture-based upstream processing. Bioprocess Int 7(S1):18–23

Eibl R, Eibl D (2009b) Application of disposable bag bioreactors in tissue engineering and for the production of therapeutic agents. Adv Biochem Eng Biotechnol 112:183–207

Eibl R, Eibl D (2010) Single-use bioreactors: an overview. In: Eibl R, Eibl D (eds) Single-use technology in biopharmaceutical manufacture. Hoboken, NJ, USA: John Wiley & Sons, pp 33–51

Eibl R, Kaiser S, Lombriser R, Eibl D (2010a) Disposable bioreactors: the current state-of-the-art and recommended applications in biotechnology. Appl Microbiol Biotechnol 86:41–49

Eibl R, Werner S, Eibl D (2010b) Bag bioreactor based on wave-induced motion: characteristics and applications. Adv Biochem Eng Biotechnol 115:55–87

Eibl R, Steiger N, Wellnitz S, Vicente T, John C, Eibl D (2013) Fast single-use VLP vaccine productions based on insect cells and the baculovirus expression vector system: influenza as case study. Adv Biochem Eng Biotechnol

Eibl R, Löffelholz C, Eibl D (2014a) Disposable bioreactors for inoculum production and protein expression. Methods Mol Biol 1104:265–284

Eibl R, Steiger N, Fritz C, Eisenkrätzer D, Bär J, Müller D, Eibl D (2014) Standardized cell culture test for the early identification of critical films for CHO cell lines and chemically defined culture media. DECHEMA, Frankfurt a.M. ISBN 978-3-89746-149-9

Falkenberg FW (1998) Production of monoclonal antibodies in the miniPERMTM bioreactor: comparison with other hybridoma culture methods. Res Immunol 149:560–570

Farouk A, Moncaubig F (2011) Engineering analysis of mixing in ATMI's bioreactors using Computational fluid dynamics. Poster presented at 22nd ESACT meeting, Vienna. Available online. http://www.atmi.com/ls-assets/pdfs/bioreactors/padreactor/Integrity_Padreactor_Poster_Esact_Digital_A4.pdf. Last accessed 27 Jan 2014

Fernald A, Pisania A, Abdelgadir E, Milling J, Marvell T, Steininger B (2009) Scale-up and comparison studies evaluating disposable bioreactors and probes. Biopharm Int:16

Fietz F (2013) Evaluierung eines neuen Abgasanalysators für Applikationen in der Zellkultur. Master thesis (unpublished), Anhalt University of Applied Sciences

Fritzsche M, Barreiro CG, Hitzmann B, Scheper T (2007) Optical pH sensing using spectral analysis. Sensor Actuat B Chem 128:133–137

Furey J (2007) Disposable large-scale pressure sensors. Genet Eng Biotechnol News 27

Garcia-Ochoa F, Gomez E (2009) Bioreactor scale-up and oxygen transfer rate in microbial processes: an overview. Biotechnol Adv 27:153–176

Genzel Y, Behrendt I, König S, Sann H, Reichl U (2004) Metabolism of MDCK cells during cell growth and influenza virus production in large-scale microcarrier culture. Vaccine 22: 2202–2208

Genzel Y, Fischer M, Reichl U (2006) Serum-free influenza virus production avoiding washing steps and medium exchange in large-scale microcarrier culture. Vaccine 24:3261–3272

Genzel Y, Dietzsch C, Rapp E, Schwarzer J, Reichl U (2010) MDCK and Vero cells for influenza virus vaccine production: a one-to-one comparison up to lab-scale bioreactor cultivation. Appl Microbiol Biotechnol 88:461–475

George M, Farooq M, Dang T, Cortes B, Liu J, Maranga L (2010) Production of cell culture (MDCK) derived live attenuated influenza vaccine (LAIV) in a fully disposable platform process. Biotechnol Bioeng 106:906–917

Glindkamp A, Riechers D, Rehbock C, Hitzmann B, Scheper T, Reardon KF (2010) Sensors in disposable bioreactors status and trends. In: Eibl R, Eibl D (eds) Disposable bioreactors,

vol 115, Advances in biochemical engineering/biotechnology. Springer, Berlin/Heidelberg, pp 145–169
Godoy-Silva R, Mollet M, Chalmers JJ (2009) Evaluation of the effect of chronic hydrodynamical stresses on cultures of suspensed CHO-6E6 cells. Biotechnol Bioeng 102:1119–1130
Gossain V, Mirro R (2010) Linear scale-up of cell cultures. Bioproc Int 8:56–62
Gossain V, Mirro R, Emerson EJ, Kedzierski S (2010) Hybrid system aims to streamline cell culture. Genet Eng Biotechnol News 30
Hahn T (2013) Practical applications of single-use technology for the production of VLP and nanoparticle vaccines. In: Eibl R, Eibl D (eds) BioTech2013 Single-use technology in biopharmaceutical manufacture. Wädenswil
Hammond M, Nunn H, Rogers G, Lee H, Marghitoiu A-L, Perez L, Nashed-Samuel Y, Anderson C, Vandiver M, Kline S (2013) Identification of a leachable compound detrimental to cell growth in single-use bioprocess containers. PDA J Pharm Sci Technol 67:123–134
Hanson MA, Brorson KA, Moreira AR, Rao G (2009) Comparisons of optically monitored small-scale stirred tank vessels to optically controlled disposable bag bioreactors. Microb Cell Fact 8:44
Hatton T, Barnett S, Rashid K (2012) CHO cell culture with single-use new Brunswick™ CelliGen® BLU Packed-Bed Fibra-Cel® Basket. Application note no. AA254. Eppendorf. Available online. http://newbrunswick.eppendorf.com/fileadmin/nbs/data/pdf/AA254_CHO_culture_BLU_Fibra-Cel.pdf. Last accessed 27 Jan 2014
Heidemann R, Mered M, Wang DQ, Gardner B, Zhang C, Michaels J, Henzler H-J, Abbas N, Konstantinov K (2002) A new seed-train expansion method for recombinant mammalian cell lines. Cytotechnology 38:99–108
Henzler H-J, Kauling DJ (1993) Oxygenation of cell cultures. Bioprocess Biosyst Eng 9:61–75
Hewitt CJ, Lee K, Nienow AW, Thomas RJ, Smith M, Thomas CR (2011) Expansion of human mesenchymal stem cells on microcarriers. Biotechnol Lett 33:2325–2335
Hildinger M, Wurm F, Stettler M, Dejesus M (2009) Cell cultivation and production of recombinant proteins by means of an orbital shake bioreactor system with disposable bags at the 1,500 liter scale. Patent US2009/0233334A1
Hirschel M (2011) Novel uses for hollow fiber bioreactors. Genet Eng Biotechnol News 31:42–44
Ho SC, Tong YW, Yang Y (2013) Generation of monoclonal antibody-producing mammalian cell lines. Pharm Bioproc 1:71–87
Hollyman D, Stefanski J, Przybylowski M, Bartido S, Borques-Ojeda O, Taylor C, Yeh R, Capacio V, Olszewska M, Hosey J, Sadelain M, Brentjens RJ, Riviéere J (2009) Manufacturing validation of biologically functional T cells targeted to CD 19 antigen for autologous adoptive cell therapy. J Immunother 32:169–180
Hopkinson J (1985) Hollow fiber cell culture systems for economical cell-product manufacturing. Bio/Technology 3:225–230
Horvath B, Tsang VL, Lin W, Dai XP, Kunas K, Frank G (2013) A generic growth test method for improving quality control of disposables in industrial cell culture. Biopharm Int 23:34–41
Hu AY-C, Weng T-C, Tseng Y-F, Chen Y-S, Wu C-H, Hsiao S, Chou A-H, Chao H-J, Gu A, Wu S-C, Chong P, Lee M-S (2008) Microcarrier-based MDCK cell culture system for the production of influenza H5N1 vaccines. Vaccine 26:5736–5740
Hui M (2009) A method to increase dissolved oxygen in a culture vessel. Patent EP2021459 A1
Hundt B, Best C, Schlawin N, Kassner H, Genzel Y, Reichl U (2007) Establishment of a mink enteritis vaccine production process in stirred-tank reactor and Wave Bioreactor microcarrier culture in 1–10 L scale. Vaccine 25:3987–3995
Imseng N (2011) Biomass and terpenoid production of Nicotiana tabacum hairy roots in single-use bioreactors. Master thesis (unpublished), Zurich University of Applied Sciences
Jia Q, Li H, Hui M, Hui N, Joudi A, Rishton G, Bao L, Shi M, Zhang X, Luanfeng L, Xu J, Leng G (2008) A bioreactor system based on a novel oxygen transfer method. Bioprocess Int 6:66–78

Jing D, Sunil N, Punreddy S, Aysola M, Kehoe D, Murrel J, Rook M, Niss K (2013) Growth kinetics of human mesenchymal stem cells in a 3-L single-use stirred-tank bioreactor. Biopharm Int 26:28–38

Josefsberg JO, Buckland B (2012) Vaccine process technology. Biotechnol Bioeng 109: 1443–1460

Jossen V, Kaiser SC, Schirmaier C, Greller G, Tappe A, Eibl D, Siehoff A, van den Bos C, Eibl R (2014) Design and qualification of the ideal single-use bioreactor for the expansion of human mesenchymal stem cells at benchtop scale. Pharm Bioproc (in peer-review)

Junker BH (2004) Scale-up methodologies for *Escherichia coli* and yeast fermentation processes. J Biosci Bioeng 97:347–364

Kadarusman J, Bhatia R, McLaughlin J, Lin WR (2005) Growing cholesterol-dependent NS0 myeloma cell line in the wave bioreactor system: overcoming cholesterol-polymer interaction by using pretreated polymer or inert fluorinated ethylene propylene. Biotechnol Prog 21: 1341–1346

Kaiser SC (2009) Theoretische und experimentelle Untersuchungen zur Bestimmung der Mischzeit und des Sauerstotransfers in Bioreaktoren. Master thesis (unpublished), Anhalt University of Applied Sciences

Kaiser SC, Löffelholz C, Werner S, Eibl D (2011a) CFD for characterizing standard and single-use stirred cell culture bioreactors. In: Minin IV, Minin OV (eds) Computational Fluid Dynamics. InTech, pp 97–122

Kaiser SC, Eibl R, Eibl D (2011b) Engineering characteristics of a single-use stirred bioreactor at bench-scale: the Mobius Cell Ready 3L bioreactor as a case study. Eng Life Sci 11:359–368

Kaiser S, Jossen V, Schirmaier C, Eibl D, Brill S, van den Bos C, Eibl R (2013) Fluid flow and cell proliferation of mesenchymal adipose-derived stem cells in small-scale, stirred, single-use bioreactors. Chem Ing Tech 85:95–102

Kamen AA, Bédard C, Tom R, Perret S, Jardin B (1996) On-line monitoring of respiration in recombinant-baculovirus infected and uninfected insect cell bioreactor cultures. Biotechnol Bioeng 50:36–48

Kauling J, Brod H, Jenne M, Waldhelm A, Langer U, Bödeker B (2013) Novel, rotary oscillated, scalable single-use bioreactor technology for the cultivation of animal cells. Chem Ing Tech 85:127–135

Kensy F, Zimmermann HF, Knabben I, Anderlei T, Trauthwein H, Dingerdissen U, Büchs J (2005) Oxygen transfer phenomena in 48-well microtiter plates: determination by optical monitoring of sulfite oxidation and verification by real-time measurement during microbial growth. Biotechnol Bioeng 89:698–708

Kilian R (2013) Managing contamination risk while maintaining quality in cell-therapy manufacturing. Bioproc Int 11:26–29

Kim JC, Seong JH, Lee B, Hashimura Y, Groux D, Oh DJ (2013) Evaluation of a novel pneumatic bioreactor system for culture of recombinant Chinese hamster ovary cells. Biotechnol Bioproc Eng 18:801–807

Kittredge A, Gowda S, Ring J, Thiel K, Simler J, Hansen A, Cieciuch J, Mumira J, Dinn L, Tran C, Burdick JA, Rapiejko, PJ (2011) Characterization and performance of the Mobius® CellReady 200 L bioreactor system: the next generation of single-use bioreactors. Poster presented at 22nd ESACT meeting, Vienna. Available online. http://www.millipore.com/publications.nsf/a73664f9f981af8c852569b9005b4eee/f57e3666e9be6877852578b90049bf73/$FILE/ps32320000_EMD.pdf. Last accessed 24 Jan 2014

Klimant I (2003) Method and device for referencing fluorescence intensity signals. Patent US 6602716 B1

Klöckner W, Gacem R, Anderlei T, Raven N, Schillberg S, Lattermann C, Büchs J (2013) Correlation between mass transfer coefficient kLa and relevant operating parameters in cylindrical disposable shaken bioreactors on a bench-to-pilot scale. J Biol Eng 7:28

Knazek RA, Gullino PM, Kohler PO, Dedrick RL (1972) Cell culture on artificial capillaries: an approach to tissue growth in vitro. Science 178:65–67

Knevelman C, Hearle DC, Osman JJ, Khan M, Dean M, Smith M, Aiyedebinu A, Cheung K (2002) Characterization and operation of a disposable bioreactor as a replacement for conventional steam-in-place inoculum bioreactors for mammalian cell culture processes. Abstr Pap Am Chem Soc 224:U233

Kumaresan T, Joshi JB (2006) Effect of impeller design on the flow pattern and mixing in stirred tanks. Chem Eng J 115:173–193

Kunas KT, Papoutsakis ET (1990) Damage mechanisms of suspended animal cells in agitated bioreactors with and without bubble entrainment. Biotechnol Bioeng 36:476–483

Lai S-W, Hou Y-J, Che C-M, Pang H-L, Wong K-Y, Chang CK, Zhu N (2004) Electronic spectroscopy, photophysical properties, and emission quenching studies of an oxidatively robust perfluorinated platinum porphyrin. Inorg Chem 43:3724–3732

Langer ES (2011) Perfusion bioreactors are making a comeback, but industry misperceptions persist. Bioproc J 9(2):49–52

Langer ES (2012) Ninth annual report and survey of biopharmaceutical manufacturing capacity and production. BioPlan Associates, 495 pages, www.bioplanassociates.com

Langheinrich C, Nienow AW, Eddleston T, Stevenson NC, Emery AN, Clayton TM, Slater NKH (2002) Oxygen transfer in stirred bioreactors under animal cell culture conditions. Food Bioprod Proc 80:39–44

Lee B, Langer E, Zheng R (2010) Next-generation single-use bioreactor technology and the future of biomanufacturing: a summary from the manufacturer's and user' perspective. In: Eibl R, Eibl D (eds) Single-use technology in biopharmaceutical manufacture. Hoboken, NJ, USA: John Wiley & Sons, pp 183–195

Legmann R, Schreyer HB, Combs RG, McCormick EL, Russo AP, Rodgers ST (2009) A predictive high-throughput scale-down model of monoclonal antibody production in CHO cells. Biotechnol Bioeng 104:1107–1120

Lehmann K, Paradies M, Haavisto E, Beyer S, Vuolanto A, Lipinsk K (2013) iCELLis fixed-bed bioreactor system for the production of oncolytic adenovirus (CGTG-102) with A549 cells. Appl Note

Lennaertz A, Knowles S, Drugmand J-C, Castillo J (2013) Viral vector production in the Integrity® iCELLis® single-use fixed-bed bioreactor, from bench-scale to industrial scale. BMC Proc 7:P59

Letellier B, Xuereb C, Swaels P, Hobbes P, Bertrand J (2002) Scale-up in laminar and transient regimes of a multi-stage stirrer, a CFD approach. Chem Eng Sci 57:4617–4632

Li C-Y, Zhang X-B, Han Z-X, Akermark B, Sun L, Shen G-L, Yu R-Q (2006) A wide pH range optical sensing system based on a sol-gel encapsulated amino-functionalized corrole. Analyst 131:388–393

Liepe F, Sperling R, Jembere S (1998) Rührwerke – Theoretische Grundlagen, Auslegung und Bewertung. Eigenverlag FH Anhalt, Köthen

Lindner P, Endres C, Bluma A, Höpfner T, Glindkamp A, Haake C, Landgrebe D, Riechers D, Baumfalk R, Hitzmann B, Scheper T, Reardon KF (2010) Disposable sensor systems. In: Eibl R, Eibl D (eds) Single-use technology in biopharmaceutical manufacture. Hoboken, NJ, USA: John Wiley & Sons, pp 67–81

Löffelholz C (2013) CFD als Instrument zur bioverfahrenstechnischen Charakterisierung von single-use Bioreaktoren und zum Scale-up für Prozesse zur Etablierung und Produktion von Biotherapeutika. PhD thesis, Brandenburg University of Technology

Löffelholz C, Kaiser SC, Werner S, Eibl D (2010) CFD as tool to characterize single-use bioreactors. In: Eibl R, Eibl D (eds) Single-use technology in biopharmaceutical manufacture. Hoboken, NJ, USA: John Wiley & Sons, pp 264–279

Löffelholz C, Husemann U, Greller G, Meusel W, Kauling J, Ay P, Kraume M, Eibl R, Eibl D (2013a) Bioengineering parameters for single-use bioreactors: overview and evaluation of suitable methods. Chem Ing Tech 85:40–56

Löffelholz C, Kaiser SC, Kraume M, Eibl R, Eibl D (2013b) Dynamic single-use bioreactors used in modern liter- and m(3)- scale biotechnological processes: engineering characteristics and scaling up. Adv Biochem Eng Biotechnol 138:1–44

Magnusson A-C, Lundström T, Lundgren M (2011) Optimization of conditions for producing influenza virus in cell culture using single-use products. Bioproc Int 9:112–113

Marx U (1998) Membrane-based cell culture technologies: a scientifically and economically satisfactory alternative to malignant ascites production for monoclonal antibodies. Res Immunol 149:557–559

McGlothlen M, Jing D, Martin C, Phillips M, Shaw R (2013) Use of microcarriers in the Mobius® Cell Ready bioreactors to support growth of adherent cells. BMC Proc 7:95–97

Merten OW, Cruz PE, Rochette C, Geny-Fiamma C, Bouquet C, Gonçalves D, Danos O, Carrondo MJ (2001) Comparison of different bioreactor systems for the production of high titer retroviral vectors. Biotechnol Prog 17:326–335

Meuwly F, Loviat F, Ruffieuc PA, Bernard AR, Kadouri A, von Stockar U (2006) Oxygen supply for CHO cells immobilized on a packed-bed of Fibra-Cel disks. Biotechnol Bioeng 93:791–800

Meuwly F, Ruffieux P, Kadouri A, von Stockar U (2007) Packed-bed bioreactors for mammalian cell culture: bioprocess and biomedical applications. Biotechnol Adv 25:45–56

Micheletti M, Barrett T, Doig SD, Baganz F, Levy MS, Woodley JM, Lye GJ (2006) Fluid mixing in shaken bioreactors: implications for scale-up predictions from microliter-scale microbial and mammalian cell cultures. Chem Eng Sci 61:2939–2949

Mills A, Chang Q (1993) Fluorescence plastic thin-film sensor for carbon dioxide. Analyst 118: 839–843

Mills A, Chang Q, McMurray N (1992) Equilibrium studies on colorimetric plastic film sensors for carbon dioxide. Anal Chem 64:1383–1389

Minow B, de Witt H, Knabben I (2013) Fast track API manufacturing from shake flask to production scale using a 1000-L single-use facility. Chem Ing Tech 85:87–94

Mollet M, Godoy-Silva R, Berdugo C, Chalmers JJ (2007) Acute hydrodynamic forces and apoptosis: a complex question. Biotechnol Bioeng 98:772–788

Moncaubeig F (2013) Simpler and more efficient viral vaccine manufacturing. Bioproc Int 11: 8–11

Müller M (2010) Realisierung eines zweistufigen Prozesses zur Plantibody-Produktion mit *BY-2*-Suspensionszellen im AppliFlex®-Bioreaktor. Bachelor thesis (unpublished), Anhalt University of Applied Sciences

Muller N, Girard P, Hacker DL, Jordan M, Wurm FM (2005) Orbital shaker technology for the cultivation of mammalian cells in suspension. Biotechnol Bioeng 89:400–406

Munkholm C, Walt DR, Milanovich FP (1988) A fiber-optic sensor for CO_2 measurement. Talanta 35:109–112

Negrete A, Kotin RM (2007) Production of recombinant adeno-associated vectors using two bioreactor configurations at different scales. J Virol Methods 145:155–161

Nienow AW (1997) On impeller circulation and mixing effectiveness in the turbulent flow regime. Chem Eng Sci 52:2557–2565

Nienow AW (2006) Reactor engineering in large scale animal cell culture. Cytotechnology 50: 9–33

Noack U, De Wilde D, Verhoeye F, Balbirnie E, Kahlert W, Adams T, Greller G, Reif O-W (2010) Single-use stirred tank reactor BIOSTAT CultiBag STR: characterisation and applications. In: Eibl R, Eibl D (eds) Single-use technology in biopharmaceutical manufacture. Hoboken, NJ, USA: John Wiley & Sons, pp 225–240

Olmer R, Kropp C, Huether-Franken C, Zweigerdt R (2013) Scalable expansion of human pluripotent stem cells in Eppendorf BioBLU® 0.3 Single-use bioreactors (Application note no. 292)

Oncül A, Kalmbach A, Genzel Y, Reichl U, Thévenin D (2009) Characterization of flow conditions in 2 L and 20 L wave bioreactors using computational fluid dynamics. Biotechnol Prog 26:101–110

Oosterhuis NMG, van der Heiden P (2010) Mass transfer in the CELL-tainer® disposable bioreactor. In: Noll T (ed) Cells and culture. Proceedings of the 20th ESACT Meeting, Dresden, Germany, vol 4. Springer Science+Business Media, pp 371–373

Oosterhuis NM, Neubauer P, Junne S (2013) Single-use bioreactors for microbial cultivation. Pharm Bioproc 1:167–177

Ott KD (2011) Are single-use technologies changing the game? Bioproc Int 9(Suppl 2):48–51

Paldus BA, Selker MD (2010) Bioinformatics and single use. In: Eibl R, Eibl D (eds) Single-use technology in biopharmaceutical manufacture. Hoboken, NJ, USA: John Wiley & Sons, pp 83–90

Palomares LA, Ramírez OT (2009) Challenges for the production of virus-like particles in insect cells: the case of rotavirus-like particles. Biochem Eng J 45:158–167

Patel G, Fettig M, Szczypka M (2012) SoloHill microcarriers in a 25-L PadReactor™ single-use bioreactor. Bioproc Int 10:22

Patwardhan AW (2001) Prediction of flow characteristics and energy balance for a variety of downflow impellers. Ind Eng Chem Res 40:3806–3816

Patwardhan AW, Joshi JB (1999) Relation between flow pattern and blending in stirred tanks. Ind Eng Chem Res 38:3131–3143

Peter CP, Suzuki Y, Büchs J (2006) Hydromechanical stress in shake flasks: correlation for the maximum local energy dissipation rate. Biotechnol Bioeng 93:1164–1176

Platas Barradas O, Jandt U, Da Minh Phan L, Villanueva ME, Schaletzky M, Rath A, Freund S, Reichl U, Skerhutt E, Scholz S, Noll T, Sandig V, Pörtner R, Zeng A-P (2012) Evaluation of criteria for bioreactor comparison and operation standardization for mammalian cell culture. Eng Life Sci 12:518–528

Qualitz J (2009) Using fluorescence-based sensing to accelerate process development. Biopharm Int 22:50

Rafiq QA, Coopman K, Hewitt CJ (2013) Scale-up of human mesenchymal stem cell culture: current technologies and future challenges. Curr Opin Chem Eng 2:8–16

Rao G, Kostov Y, Moreira A, Frey D, Hanson M, Jornitz M, Reif O-W, Baumfalk R, Qualitz J (2009) Non-invasive sensors as enablers of "smart" disposables. Bioproc Int 7(S1):24–27

Ries C (2008) Untersuchung zum Einsatz von Einwegbioreaktoren für die auf Insektenzellen basierte Produktion von internen und externen Proteinen. Diploma thesis (unpublished), Zurich University of Applied Sciences

Rodriguez R, Castillo J, Giraud S (2010) Demonstrated performance of a disposable bioreactor with an anchorage-dependent cell line. Bioproc Int 8:74–77

Rowley J, Abraham E, Campbell A, Brandwein H, Oh S (2012) Meeting lot-size challenges of manufacturing adherent cells for therapy. Bioproc Int 10:16–22

Schirmaier C, Jossen V, Kaiser SC, Jürgerkes F, Brill S, Safavi-Nab A, Siehoff A, van den Bos C, Eibl D, Eibl R (2014) Scale-up of mesenchymal adipose tissue-derived stem cell production in stirred single-use bioreactors under low-serum conditions. Eng Life Sci 14(3):292–303

Schmid G (1996) Insect cell cultivation: growth and kinetics. Cytotechnology 20:43–56

Schneditz D, Kenner T, Heimel H, Stabinger H (1989) A sound-speed sensor for the measurement of total protein-concentration in disposable, blood-fused tubes. J Acoust Soc Am 86: 2073–2080

Schouwenberg JE, van der Velden-de Groot T, Blueml G (2010) Vaccine production utilizing the potential of microcarriers in disposable bioreactor. In: Noll T (ed) Cells and culture. ESACT proceedings. Springer, pp 795–801

Schultz JB, Giroux D (2011) 3-L to 2,500-L single-use bioreactors, state of the art solutions for cell culture processes and applications. Bioproc Int 9:120

Schwander E, Rasmussen H (2005) Scalable, controlled growth of adherent cells in disposable multilayer format. Genet Eng Biotechnol News 25:29

Shiragami N (1997) Effect of shear rate on hybridoma cell metabolism. Bioproc Eng 16:345–347

Shukla AA, Gottschalk U (2013) Single-use disposable technologies for biopharmaceutical manufacturing. Trends Biotechnol 31:147–154

Shukla AA, Mostafa S, Wilson M, Lange D (2012) Vertical integration of disposables in biopharmaceutical drug substance manufacturing. Bioproc Int 10:34–47

Singh V (1999) Disposable bioreactor for cell culture using wave-induced agitation. Cytotechnology 30:149–158

Singh V (2001) Method for culturing cells using wave-induced agitation. Patent US 6190913 B1

Smelko JP, Wiltberger KR, Hickman EF, Morris BJ, Blackburn TJ, Ryll T (2011) Performance of high intensity fed-batch mammalian cell cultures in disposable bioreactor systems. Biotechnol Prog 27:1358–1364

Smith CG, Greenfield PF (1992) Mechanical agitation of hybridoma suspension cultures: metabolic effects of serum, pluronic F68, and albumin supplements. Biotechnol Bioeng 40:1045–1055

Spichiger S, Spichiger-Keller UE (2010) New single-use sensors for online measurement of glucose and lactate: the answer to the PAT initiative. In: Eibl R, Eibl D (eds) Single-use technology in biopharmaceutical manufacture. Hoboken, NJ, USA: John Wiley & Sons, pp 264–279

Stettler M, Zhang X, Anderlei T, De Jesus M, Lefebvre P, Hacker DL, Wurm FM (2010) Development of pilot-scale orbital shake bioreactors: ideal for cost-effective and efficient transient gene expression. In: Noll T (ed) ESACT proceedings, vol 4. Springer, pp 183–186

Sun B, Yu X, Kong W, Sun S, Yang P, Zhu C, Zhang H, Wu Y, Chen Y, Shi Y, Zhang X, Jiang C (2013) Production of influenza H_1N_1 vaccine from MDCK cells using a novel disposable packed-bed bioreactor. Appl Microbiol Biotechnol 97:1063–1070

Surman C, Potyrailo RA, Morris WG, Wortley T, Vincent M, Diana R, Pizzi V, Carter J, Gach G (2011) Temperature-independent passive RFID pressure sensors for single-use bioprocess components. In: IEEE Int. Conf. RFID, Orlando, Florida, pp 78–84

Sutlu T, Stellan B, Gilljam M, Quezada HC, Nahi H, Gahrton G, Alici E (2010) Clinical-grade, large-scale, feeder-free expansion of highly active human natural killer cells for adoptive immunotherapy using an automated bioreactor. Cytotherapy 12:1044–1055

Tan R-K, Eberhard W, Büchs J (2011) Measurement and characterization of mixing time in shake flasks. Chem Eng Sci 66:440–447

Tang YJ, Ohashi R, Hamel JFP (2007) Perfusion culture of hybridoma cells for hyperproduction of IgG(2a) monoclonal antibody in a wave bioreactor-perfusion culture system. Biotechnol Prog 23:255–264

Tao Y, Shih J, Sinacore M, Ryll T, Yusuf-Makagiansar H (2011) Development and implementation of a perfusion-based high cell density cell banking process. Biotechnol Prog 27:824–829

Thomassen YE, van der Welle JE, van Eikenhorst G, van der Pol LA, Bakker WAM (2012) Transfer of an adherent Vero cell culture method between two different rocking motion type bioreactors with respect to cell growth and metabolic rates. Process Biochem 47:288–296

Timmins NE, Kiel M, Günther M, Heazlewood C, Doran MR, Brooke G, Atkinson K (2012) Closed system isolation and scalable expansion of human placental mesenchymal stem cells. Biotechnol Bioeng 109:1817–1826

Tissot S, Farhat M, Hacker DL, Anderlei T, Kühner M, Comninellis C, Wurm F (2010) Determination of a scale-up factor from mixing time studies in orbitally shaken bioreactors. Biochem Eng J 52:181–186

Tissot S, Oberbek A, Reclari M, Dreyer M, Hacker DL, Baldi L, Farhat M, Wurm FM (2011a) Efficient and reproducible mammalian cell bioprocesses without probes and controllers? N Biotechnol 28(4):382–390

Tissot S, Reclari M, Quinodoz S, Dreyer M, Monteil DT, Baldi L, Hacker DL, Farhat M, Discacciati M, Quarteroni A, Wurm FM (2011b) Hydrodynamic stress in orbitally shaken bioreactors. BMC Proc 5(Suppl 8):P39

Tran CA, Burton L, Russom D, Wagner JR, Jensen MC, Forman SJ, DiGiusto DL (2007) Manufacturing of large numbers of patent-specific T cells for adoptive immunotherapy: an approach to improving product safety, composition, and production capacity. J Immunother 30:644–654

Trounson A, Thakar RG, Lomax G, Gibbons D (2011) Clinical trials for stem cell therapies. BMC Med 9:52

Uttamlal M, Walt DR (1995) A fiber-optic carbon dioxide sensor for fermentation monitoring. Nat Biotechnol 13:597–601
van den Bos C, Keefe R, Schirmaier C, McCaman M (2014) Therapeutic human cells: manufacture for cell therapy/regenerative medicine. Adv Biochem Eng Biotechnol 38:61–97
van't Riet KV (1979) Review of measuring methods and results in mass transfer in stirred vessels. Ind Eng Chem Proc Des Dev 18:357–364
Venkat RV, Chalmers JJ (1996) Characterization of agitation environments in 250 ml spinner vessel, 3 L, and 20 L reactor vessels used for animal cell microcarrier culture. Cytotechnology 22:95–102
Vicente T, Roldão A, Peixoto C, Carrondo MJT, Alves PM (2011) Large-scale production and purification of VLP-based vaccines. J Invertebr Pathol 107(Suppl):S42–S48
Vorlop J, Lehmann J (1988) Scale-up of bioreactors for fermentation of mammalian cell cultures, with special reference to oxygen supply and microcarrier mixing. Chem Eng Technol 11:171–178
Wang L, Hu H, Yang J, Wang F, Kaisermayer C, Zhou P (2012a) High yield of human monoclonal antibody produced by stably transfected Drosophila schneider 2 cells in perfusion culture using wave bioreactor. Mol Biotechnol 52:170–179
Wang Y, Han Z-B, Song Y-P, Han ZC (2012b) Safety of mesenchymal stem cells for clinical application. Stem Cells Int 2012:652034
Weber W, Fussenegger M (2009) Insect cell-based recombinant protein production. In: Springer (ed) Cell and tissue reaction engineering. Springer, Berlin/Heidelberg, pp 263–277
Weber A, Husemann U, Chaussin S, Adams T, de Wilde D, Gerighausen S, Greller G, Fenge C (2013) Development and qualification of a scalable, disposable bioreactor for GMP-compliant cell culture. Biopharm Int Suppl 11:6–17
Wen Y, Zang R, Zhang X, Yang S-T (2012) A 24-microwell plate with improved mixing and scalable performance for high throughput cell cultures. Process Biochem 47:612–618
Werner S, Eibl R, Lettenbauer C, Röll M, Eibl D, De Jesus M, Zhang X, Stettler M, Tissot S, Bürki C, Broccard G, Kühner M, Tanner R, Baldi L, Hackera D, Wurm FM (2010a) Innovative, non-stirred bioreactors in scales from milliliters up to 1000 liters for suspension cultures of cells using disposable bags and containers – a Swiss contribution. Chimia 64:819–823
Werner S, Kraume M, Eibl D (2010b) Bag mixing systems for single-use. In: Eibl R, Eibl D (eds) Single-use technology in biopharmaceutical manufacture. Hoboken, NJ, USA: John Wiley & Sons, pp 21–32
Werner S, Olownia J, Egger D, Eibl D (2013) An approach for scale-up of geometrically dissimilar orbitally shaken single-use bioreactors. Chem Ing Tech 85:118–126
Whitford WG (2010) Single-use systems as principal components in bioproduction. Bioproc Int 8: 34–42
Whitford WG, Cadwell JJS (2009) Interest in hollow-fiber perfusion bioreactors is growing. Bioproc Int 7:54–63
Whitford WG, Fairbank A (2011) Considerations in scale-up of viral vaccine production. Bioproc Int 9:16–28
Wood J, Mahajan E, Shiratori M (2013) Strategy for selecting disposable bags for cell culture media applications based on a root-cause investigation. Biotechnol Prog 29(6):1535–1549
Xing Z, Kenty BM, Li ZJ, Lee SS (2009) Scale-up analysis for a CHO cell culture process in large-scale bioreactors. Biotechnol Bioeng 103:733–746
Yang S-T, Liu X (2013) Cell culture processes for biologics manufacturing: recent developments and trends. Pharm Bioproc 1:133–136
Yim SS, Shamlou PA (2000) The engineering effects of fluids flow on freely suspended biological macro-materials and macromolecules. Adv Biochem Eng Biotechnol 67:83–122
Zambeaux JP, Vanhamel S, Bosco F, Castillo J (2007) Disposable bioreactor. Patent EP1961606A2
Zhang H, Williams-Dalson W, Keshavarz-Moore E, Shamlou PA (2005) Computational-fluid-dynamics (CFD) analysis of mixing and gas-liquid mass transfer in shake flasks. Biotechnol Appl Biochem 41:1–8

Zhang H, Lamping SR, Pickering SCR, Lye GJ, Shamlou PA (2008a) Engineering characterisation of a single well from 24-well and 96-well microtitre plates. Biochem Eng J 40:138–149

Zhang X, Stettler M, Reif O, Kocourek A, Dejesus M, Hacker DL, Wurm FM (2008b) Shaken helical track bioreactors: providing oxygen to high-density cultures of mammalian cells at volumes up to 1000 L by surface aeration with air. N Biotechnol 25:68–75

Zhang X, Bürki C-A, Stettler M, De Sanctisc D, Perronec M, Discacciati M, Parolini N, DeJesusb M, Hacker DL, Alfio Quarteronic FMW (2009) Efficient oxygen transfer by surface aeration in shaken cylindrical containers for mammalian cell cultivation at volumetric scales up to 1000 L. Biochem Eng J 45:41–47

Zhang X, Stettler M, De Sanctis D, Perrone M, Parolini N, Discacciati M, De Jesus M, Hacker D, Quarteroni A, Wurm F (2010) Use of orbital shaken disposable bioreactors for mammalian cell cultures from the milliliter-scale to the 1,000-liter scale. Adv Biochem Eng Biotechnol 115: 33–53

Zhu H, Nienow AW, Bujalski W, Simmons MJH (2009) Mixing studies in a model aerated bioreactor equipped with an up- or a down-pumping "Elephant Ear" agitator: power, hold-up and aerated flow field measurements. Chem Eng Res Des 87:307–317

Zijlstra GM, Hoff RP, Schilderer J (2012) Process for culturing of cells. US Patent US8222001 B2

Zlokarnik M (1999) Rührtechnik – Theorie und Praxis. Springer, Berlin/Heidelberg/New York

Zouwenga R, D'Avino A, Zijlstra GM (2010) Improving productivity in bioreactors. Genet Eng Biotechnol News 30:1–4